

On the adaptive Levin method

Shukui Chen^{1*}, Kirill Serkh^{1,2*} and James Bremer^{2*}

^{1*}Department of Computer Science, University of Toronto.

²Department of Mathematics, University of Toronto.

*Corresponding author(s). E-mail(s): bremer@math.toronto.edu;

Abstract

The Levin method is a well-known technique for evaluating oscillatory integrals, which operates by solving a certain ordinary differential equation in order to construct an antiderivative of the integrand. It was long believed that this approach suffers from “low-frequency breakdown,” meaning that the accuracy of the calculated value of the integral deteriorates when the integrand is only slowly oscillating. Recently presented experimental evidence, however, suggests that if a Chebyshev spectral method is used to discretize the differential equation and the resulting linear system is solved via a truncated singular value decomposition, then no low-frequency breakdown occurs. Here, we provide a proof that this is the case, and our proof applies not only when the integrand is slowly oscillating, but even in the case of stationary points. Our result puts adaptive schemes based on the Levin method on a firm theoretical foundation and accounts for their behavior in the presence of stationary points. We go on to point out that by combining an adaptive Levin scheme with phase function methods for ordinary differential equations, a large class of oscillatory integrals involving special functions, including products of such functions and the compositions of such functions with slowly-varying functions, can be easily evaluated without the need for symbolic computations. Finally, we present the results of numerical experiments which illustrate the consequences of our analysis and demonstrate the properties of the adaptive Levin method.

1 Introduction

The Levin method, which was introduced in [1], is a classical technique for evaluating integrals of the form

$$\int_a^b \exp(ig(x))f(x) dx, \quad (1)$$

where f is a slowly varying, g is real-valued and slowly varying and g' is of large magnitude. It operates by solving the ordinary differential equation

$$p'(x) + ig'(x)p(x) = f(x) \quad (2)$$

in order to find a function p such that

$$\frac{d}{dx} (p(x) \exp(ig(x))) = f(x) \exp(ig(x)). \quad (3)$$

The value of the integral (1) is then equal to

$$p(b) \exp(ig(b)) - p(a) \exp(ig(a)). \quad (4)$$

Under the assumptions made above, (2) admits a slowly-varying solution p_0 , which means that (1) can be computed rapidly. Moreover, although the differential operator

$$L[p](x) = p'(x) + ig'(x)p(x) \quad (5)$$

appearing on the left-hand side of (2) has a one-dimensional nullspace consisting of all multiples of the function $\eta(x) = \exp(-ig(x))$, the equation (2) can still be solved accurately via a spectral collocation method if some care is taken. In particular, as long as the chosen grid of collocation nodes is dense enough to resolve f and g' , but not sufficiently dense to resolve η , the matrix discretizing the differential operator L will be well-conditioned and inverting it will result in a high-accuracy approximation of the slowly varying solution p_0 .

When the magnitude of g' is sufficiently small, any grid of collocation nodes dense enough to resolve f and g' will also resolve η . As a consequence, the corresponding spectral discretization of L will have a small singular value and numerical difficulties can arise in the course of solving (2). This phenomenon is known as “low-frequency breakdown,” and it was long believed to be a significant limitation of Levin methods. The recent articles [2, 3] present experimental evidence showing that, when Chebyshev spectral methods are used to discretize the differential equation (2) and the resulting linear system is solved via a truncated singular value decomposition, no low-frequency breakdown seems to occur.

Here, we prove that this is the case. We first show that, when g' is nonvanishing, the Levin equation admits a well-behaved solution that can be approximated by a polynomial expansion at a cost which depends on a measure of the complexity of f , g' and the inverse function g^{-1} of g , as well as the ratio of the maximum and minimum values of g' , but not on the magnitude of g' . This

result improves on the those presented in both original Levin paper [1] and its follow-up [4] by handling the case in which g' is of positive, but arbitrarily small, magnitude and by explicitly showing that the cost of representing the well-behaved solution of the Levin equation via a polynomial expansion is independent of the magnitude of g' (note that the assumptions made in both [1] and [4] fail to hold when g' is of sufficiently small positive magnitude). We then consider the case in which g' is of small magnitude, possibly with zeros. In this event, g need not be invertible, but we show that the Levin equation nonetheless admits a well-behaved solution, and that this solution can be approximated by a polynomial expansion at a cost which decreases with the magnitude of g' . We use these two results to prove that, when the Levin equation is discretized via a Chebyshev spectral collocation method and the resulting linear system is solved using a truncated singular value decomposition, high accuracy is obtained regardless of the magnitude of g' and whether or not g' has zeros.

One implication of the absence of low-frequency breakdown is that the Levin method can be used as the basis of an adaptive integration scheme — since adaptive subdivision reduces the effective magnitude of g' , such an approach requires that the method remain accurate regardless of the magnitude of g' . An adaptive Levin scheme was proposed by Moylan [5] before the absence of low-frequency breakdown was observed in [2, 3]. Moylan's scheme is based on a more general version of the Levin method introduced in [6]. In particular, the integrand is of the form

$$\int_a^b \mathbf{w}(x) \cdot \mathbf{f}(x) dx \quad (6)$$

with $\mathbf{f}: [a, b] \rightarrow \mathbb{C}^n$ slowly-varying and $\mathbf{w}: [a, b] \rightarrow \mathbb{C}^n$ a solution of a system of ordinary differential equations

$$\mathbf{w}'(x) = \mathbf{A}(x)\mathbf{w}(x) \quad (7)$$

whose coefficient matrix $\mathbf{A}: [a, b] \rightarrow \mathbb{C}^{n \times n}$ is also slowly-varying. The scheme of [6] operates by finding a slowly-varying vector field $\mathbf{F}: [a, b] \rightarrow \mathbb{C}^n$ satisfying the system of differential equations

$$\mathbf{F}'(x) + \mathbf{A}(x)^t \mathbf{F}(x) = \mathbf{f}(x) \quad (8)$$

and evaluating (6) via the formula

$$\mathbf{F}(b) \cdot \mathbf{w}(b) - \mathbf{F}(a) \cdot \mathbf{w}(a). \quad (9)$$

Moylan's algorithm adaptively decomposes the domain of an oscillatory integral and uses the above formulation of the Levin method to evaluate it over each subinterval. An implementation of this scheme using Wolfram's Mathematica package is described in [5], and experimental evidence showing that it works well in practice in the low-frequency regime, and even in the case of stationary points, is presented. However, all of the estimates discussed in [5] break down in the low-frequency regime. Moreover, the implementation of the

4 *On the adaptive Levin method*

adaptive Levin method described in [5] relies heavily on symbolic and arbitrary precision computations, including in the solution of the linear system which arises when (8) is discretized. Since that system typically becomes highly ill-conditioned at low frequencies, it is unclear how the scheme would fare if the calculations were performed in double precision arithmetic.

One ostensible advantage of the Moylan scheme over an adaptive scheme based on the original Levin formulation [1] is the great generality of the integrands which can be expressed as solutions of systems of the form (7) with slowly-varying coefficient matrices. However, most oscillators of interest are solutions of scalar differential equations of the form

$$y^{(n)}(t) + q_{n-1}(t)y^{(n-1)}(t) + \cdots + q_1(t)y'(t) + q_0(t)y(t) = 0 \quad (10)$$

whose coefficients are slowly-varying, and it is well known that such equations admit slowly-varying phase functions. More explicitly, under mild conditions on the coefficients q_0, \dots, q_{n-1} , there exist slowly-varying ψ_1, \dots, ψ_n such that

$$\{\exp(\psi_j(t)) : j = 1, \dots, n\} \quad (11)$$

is a basis in the space of solutions of (10). This observation underlies the WKB method and almost all other techniques for the asymptotic approximation of solutions of ordinary differential equations in the high-frequency regime (see, for instance, [7], [8] and [9, 10, 11]). See also [12], which contains a careful proof of the existence of slowly-varying phase functions for second order differential equations that can be extended to the case of higher order scalar equations without too much difficulty. A numerical algorithm for constructing slowly-varying functions for a scalar equations of the form (10) in time independent of frequency is described in [13]. Specialized methods for the case of second order linear ordinary differential equations are described in [14] and [15]. Because many of the oscillators of most interest satisfy second order linear ordinary differential equations (including the Bessel functions, Jacobi polynomials, spheroidal wave functions, and Hermite polynomials), the experiments of this article focus on this case and we use the algorithm of [15] in order to construct the necessary slowly-varying phase functions.

It follows from the existence of slowly-varying phase functions for scalar differential equations that an adaptive method based on Levin's original formulation suffices to evaluate a huge class of oscillatory integrals. Moreover, when explicit exponential representations of oscillators are available, integrals involving the product of two oscillators or the composition of an oscillator with a slowly-varying function can be evaluated in a straightforward fashion. This is in contrast to Moylan's adaptive scheme, which requires knowledge of a system of differential equations satisfied by whatever combination of oscillators is being considered. Moylan's scheme relies heavily on Mathematica's symbolic capabilities to derive the necessary differential equations.

The remainder of this article is structured as follows. Section 2 discusses the requisite mathematical and numerical preliminaries. Section 3 contains our

analysis showing that the Levin equation always admits a well-behaved solution. In Section 4, we use the results of Section 3 to establish that no accuracy is lost when a Chebyshev collocation scheme is used to discretize the Levin equation and the resulting system of linear equations is solved via a truncated singular value decomposition. In Section 5, we give a detailed description of the adaptive Levin method. In Section 6, we present the results of numerical experiments conducted to demonstrate the properties of the adaptive Levin method. Finally, we close with a few brief remarks in Section 7.

2 Preliminaries

2.1 Notation and conventions

We use capital script letters such as \mathcal{A} for matrices, and vectors are indicated with an overline as in \bar{x} . We denote by $L^\infty(\Omega)$ the Banach space of functions which are essentially bounded on the Lebesgue measurable subset Ω of \mathbb{R} , and by $C^n([a, b])$ the Banach space of functions $(a, b) \mapsto \mathbb{C}$ whose derivatives through order n are uniformly continuous and hence admit continuous extensions to $[a, b]$. We denote by $M([a, b])$ the Banach space of complex Radon measures on $[a, b]$, which is the dual of $C^0([a, b])$, and by $|\mu|$ the total variation of $\mu \in M([a, b])$. The notation $\|x\|_X$ is used for the norm of an element x of one of the Banach spaces X mentioned above. The Euclidean norm of a vector $\bar{x} \in \mathbb{C}^n$ is $\|\bar{x}\|$, and $\|\mathcal{A}\|$ is the $\mathbb{C}^n \rightarrow \mathbb{C}^n$ Euclidean operator norm of the $n \times n$ matrix \mathcal{A} .

We denote by $C^\infty([a, b])$ the set of functions which are infinitely differentiable and whose derivatives of all orders are uniformly continuous on (a, b) , and use $S(\mathbb{R})$ for the Schwartz space of infinitely differentiable functions whose derivatives of all orders are rapidly decaying functions. The space of tempered distributions is $S'(\mathbb{R})$. We often write $\langle \varphi, f \rangle$ for the action of the tempered distribution φ on the function $f \in S(\mathbb{R})$, although we occasionally use other notations for this when their meanings are clear. The support of $\varphi \in S'(\mathbb{R})$ is the complement of the union of all open sets U such that $\langle \varphi, f \rangle = 0$ whenever $f \in S(\mathbb{R})$ has support contained in U . The order of a tempered distribution φ is the least nonnegative integer n with the property that for each compact set $K \subset \mathbb{R}$ there exists a constant M_K such that

$$|\langle \varphi, f \rangle| \leq M_K \sup_{0 \leq k \leq n} \sup_{x \in K} |D^k f(x)| \quad (12)$$

for every function $f \in S(\mathbb{R})$ whose support is contained in K (we note that every tempered distribution has finite order). The space of tempered distributions of order n which are supported on $[a, b]$ can, of course, be identified with the dual space of $C^n([a, b])$.

We use the convention

$$\widehat{f}(\xi) = \frac{1}{2\pi} \int_{-\infty}^{\infty} f(x) \exp(-i\xi x) dx \quad (13)$$

for the Fourier transform of $f \in S(\mathbb{R})$ (this is slightly nonstandard, but quite convenient when discussing the Levin equation). Of course, $\widehat{f} \in S(\mathbb{R})$ and we have

$$f(x) = \int_{-\infty}^{\infty} \widehat{f}(\xi) \exp(i\xi x) d\xi. \quad (14)$$

We extend the Fourier transform to a mapping $S'(\mathbb{R}) \rightarrow S'(\mathbb{R})$ in the usual way, via the formula $\langle \widehat{\varphi}, g \rangle = \langle \varphi, \widehat{g} \rangle$. If φ is compactly supported on $[a, b]$, then its Fourier transform coincides with the function $\widehat{\varphi}(\xi) = \langle \varphi, \eta_{\xi} \rangle$, where $\eta_{\xi}(x) = 1/(2\pi) \exp(-ix\xi)$. The Schwartz-Paley-Wiener theorem asserts that $\widehat{\varphi}$ is entire in this case, and gives bounds on its growth at infinity. Likewise, if $\widehat{\varphi}$ is compactly supported on $[a, b]$, then φ is the entire function defined via the formula $\varphi(x) = \langle \widehat{\varphi}, \nu_x \rangle$ with $\nu_x(\xi) = \exp(i\xi x)$. If the Fourier transform of φ is supported on the finite interval $[-c, c]$, then we say that φ has bandlimit c . Note that we do not require that c be the smallest positive real number with this property.

The notation $x \lesssim y$ indicates that there is some constant C not depending on y such that $x \leq Cy$. We say that

$$f(z) = \mathcal{O}(g(z)) \quad \text{as } z \rightarrow \infty \quad (15)$$

provided there exist $M > 0$ and $C > 0$ such that

$$|f(z)| \leq C |g(z)| \quad \text{for all } z > M. \quad (16)$$

2.2 Chebyshev interpolation

We use T_n to denote the Chebyshev polynomial of degree n and

$$-1 = x_{1,k}^{\text{cheb}} < x_{2,k}^{\text{cheb}} < \dots < x_{k,k}^{\text{cheb}} = 1 \quad (17)$$

for the k -point grid of Chebyshev extremal nodes on the interval $[-1, 1]$. That is,

$$x_{j,k}^{\text{cheb}} = \cos\left(\pi \frac{k-j}{k-1}\right), \quad j = 1, \dots, k. \quad (18)$$

It is well known that

$$\begin{aligned} & \frac{2}{k-1} \sum_{j=1}^k {}'' T_n(x_{j,k}^{\text{cheb}}) T_m(x_{j,k}^{\text{cheb}}) \\ &= \begin{cases} 1 & \text{if } n = 1, \dots, k-2 \text{ and } \text{mod}(m, 2(k-1)) = n \\ 2 & \text{if } n = 0, (k-1) \text{ and } \text{mod}(m, 2(k-1)) = n \\ 0 & \text{otherwise,} \end{cases} \end{aligned} \quad (19)$$

where the double prime symbol after the summation indicates that the first and last term of the series are weighted by $1/2$ (this formula can be found, for instance, in Chapter 4 of [16]). If $f \in C^\infty([-1, 1])$, then we use $P_k[f]$ to

denote the Chebyshev expansion of the form

$$\sum_{n=0}^{k-1} a_n T_n(x) \quad (20)$$

which agrees with f at the nodes (17). It follows from (19) that the coefficients in (20) are given by

$$a_n = \begin{cases} \frac{1}{k-1} \sum_{j=1}^k {}''T_n(x_j^{\text{cheb}}) f(x_j^{\text{cheb}}) & \text{if } n = 0 \text{ or } n = k-1 \\ \frac{2}{k-1} \sum_{j=1}^k {}''T_n(x_j^{\text{cheb}}) f(x_j^{\text{cheb}}) & \text{if } n = 1, \dots, k-2. \end{cases} \quad (21)$$

The k^{th} order Chebyshev spectral differential matrix is the $k \times k$ matrix \mathcal{D}_k which maps the vector

$$\begin{pmatrix} g(x_{1,k}^{\text{cheb}}) \\ g(x_{2,k}^{\text{cheb}}) \\ \vdots \\ g(x_{k,k}^{\text{cheb}}) \end{pmatrix} \quad (22)$$

of values of an expansion of the form

$$g(x) = \sum_{n=0}^{k-1} a_n T_n(x) \quad (23)$$

at the extremal Chebyshev nodes to the vector

$$\begin{pmatrix} g'(x_{1,k}^{\text{cheb}}) \\ g'(x_{2,k}^{\text{cheb}}) \\ \vdots \\ g'(x_{k,k}^{\text{cheb}}) \end{pmatrix} \quad (24)$$

of values of the derivative of (23) at the extremal Chebyshev nodes.

If $f \in C^\infty([-1, 1])$ is infinitely differentiable, then it admits a uniformly convergent Chebyshev series

$$f(x) = \sum_{n=0}^{\infty} b_n T_n(x) \quad (25)$$

such that

$$|b_n| = \mathcal{O}\left(\frac{1}{n^m}\right) \quad \text{as } n \rightarrow \infty \quad (26)$$

for all $m \geq 1$. From (19) it is clear that the coefficients $\{b_n\}$ in (25) are related to the coefficients $\{a_n\}$ in the expansion of $P_k[f]$ through the formula

$$a_n = b_n + b_{n+2(k-1)} + b_{n+4(k-1)} + \dots \quad (27)$$

Since $|T_n(x)| \leq 1$ and $|T'_n(x)| \leq n^2$ for all $x \in [-1, 1]$, it follows from (27) that

$$\|P_k[f] - f\|_{L^\infty([-1,1])} \leq 2 \sum_{n=k}^{\infty} |b_n| \quad (28)$$

and

$$\|P_k[f]' - f'\|_{L^\infty([-1,1])} \leq 2 \sum_{n=k}^{\infty} n^2 |b_n|. \quad (29)$$

Obviously, if f is a polynomial of degree less than k , then

$$P_k[f](x) = f(x) \quad (30)$$

and

$$P_k[f'](x) = f'(x) = P_k[f]'(x). \quad (31)$$

2.3 Approximation by bandlimited functions

It will often be necessary for us to approximate a function f given on the interval $[-1, 1]$ via a “well-behaved” bandlimited function f_b . For us, well-behaved means that the $L^\infty(\mathbb{R})$ norms of f_b , its Fourier transform and the derivative of its Fourier transform are bounded by small constant multiples of the $L^\infty([-1, 1])$ norm of f . Moreover, it is desirable to minimize the bandlimit of f_b subject to these constraints.

Under various regularity assumptions on f , it is possible to prove the existence of an approximate satisfying these requirements. The following theorem, which is a slightly modified version of Theorem 1 in [17], is an example of a result of this type which holds under relatively weak regularity conditions on f .

Theorem 1 *Suppose that $f : [-1, 1] \rightarrow \mathbb{C}$ admits an infinitely differentiable extension to an open neighborhood of $[-1, 1]$. Then for each positive integer m and each real number $c > 1$, there exist a constant k depending on m but not c , and a function $f_b \in S(\mathbb{R})$ such that*

1. $\widehat{f_b}$ is supported on $[-c-2, c+2]$,
2. $\|f_b - f\|_{L^\infty([-1,1])} \leq \frac{k}{c^m}$,
3. $\|f_b(x)\|_{L^\infty(\mathbb{R})} \leq 2\|f\|_{L^\infty([-1,1])} + \frac{k}{c^m}$,
4. $\left\| \widehat{f_b}(\xi) \right\|_{L^\infty(\mathbb{R})} \leq 4\|f\|_{L^\infty([-1,1])}$ and

$$5. \left\| \widehat{f}_b'(\xi) \right\|_{L^\infty(\mathbb{R})} \leq 4 \|f\|_{L^\infty([-1,1])}.$$

Proof We let $M = \|f\|_{L^\infty([-1,1])}$ and choose $0 < \delta < 1$ such that f is infinitely differentiable on $[-1 - \delta, 1 + \delta]$ and bounded in magnitude by $2M$ there. We take T_1 to be an infinitely differentiable window function $\mathbb{R} \rightarrow \mathbb{R}$ such that $|T_1(x)| \leq 1$ for all $x \in \mathbb{R}$, $T_1(x) = 1$ for all $x \in [-1, 1]$ and $T_1(x) = 0$ for all $|x| \geq 1 + \delta$. One can construct this function quite easily using the infinitely differentiable ramp function

$$H(x) = \begin{cases} \frac{1}{2} \left(1 + \operatorname{erf} \left(\frac{x}{\sqrt{1-x^2}} \right) \right) & x \in [-1, 1] \\ 0 & |x| > 1 \end{cases} \quad (32)$$

suggested in [17]. Then $f_1(x) = f(x)T_1(x)$ is an element of the space $S(\mathbb{R})$, and so is its Fourier transform \widehat{f}_1 . Consequently, there exists a constant k_1 (depending on m) such that

$$\sup_{|\xi| \geq 1} \left| \widehat{f}_1(\xi) \right| \leq \frac{k_1}{|\xi|^{m+1}}. \quad (33)$$

Since T_1 is bounded in magnitude by 1,

$$|f_1(x)| \leq 2M \quad \text{for all } x \in \mathbb{R}. \quad (34)$$

It follows from this that

$$\left| \widehat{f}_1(\xi) \right| = \left| \frac{1}{2\pi} \int_{-1-\delta}^{1+\delta} f_1(x) \exp(-i\xi x) dx \right| \leq \frac{2}{\pi} (1 + \delta) M \leq \frac{4}{\pi} M \quad (35)$$

and

$$\left| \widehat{f}_1'(\xi) \right| = \left| \frac{-i}{2\pi} \int_{-1-\delta}^{1+\delta} f_1(x) x \exp(-i\xi x) dx \right| \leq \frac{2}{\pi} (1 + \delta)^2 M \leq \frac{8}{\pi} M \quad (36)$$

for all $\xi \in \mathbb{R}$.

Now we let T_2 be an infinitely differentiable window function such that $|T_2(x)| \leq 1$ and $|T_2'(x)| \leq 1$ for all $x \in \mathbb{R}$, $T_2(x) = 1$ for all $x \in [-c, c]$ and $T_2(x) = 0$ for all $|x| > c + 2$. Such a function can be easily constructed using the ramp function H defined in (32). We define f_b by

$$\widehat{f}_b(\xi) = \widehat{f}_1(\xi) T_2(\xi), \quad (37)$$

so that the first of the properties listed above is clearly satisfied. From (33) and the definition of T_2 , it is clear that for all $x \in [-1, 1]$,

$$\begin{aligned} |f_1(x) - f_b(x)| &= \left| \frac{1}{2\pi} \int_{-\infty}^{\infty} \widehat{f}_1(\xi) (1 - T_2(\xi)) \exp(i\xi x) d\xi \right| \\ &\leq \frac{1}{\pi} \int_{|\xi| > c} \left| \widehat{f}_1(\xi) \right| d\xi \\ &\leq \frac{2k_1}{m\pi c^m}. \end{aligned} \quad (38)$$

This inequality establishes the second of the properties of the function f_b listed above and, by combining it with (34), we obtain the third. It follows from (35), (36) and the properties of T_2 that

$$\left| \widehat{f}_b(\xi) \right| = \left| \widehat{f}_1(\xi) T_2(\xi) \right| \leq \frac{4}{\pi} M \quad (39)$$

and

$$\left| \widehat{f}_b'(\xi) \right| = \left| \widehat{f}_1'(\xi)T_2(\xi) + \widehat{f}_1(\xi)T_2'(\xi) \right| \leq \frac{4}{\pi}M + \frac{8}{\pi}M = \frac{12}{\pi}M \quad (40)$$

for all $\xi \in \mathbb{R}$. This establishes the last two of the properties of f_b listed above. \square

More precise results of this type can be given under stronger regularity assumptions on f . However, the necessary arguments are rather technical and beyond the scope of this paper. Accordingly, now that we have established the existence of a suitable bandlimited approximate under the weak condition that f admits an infinitely differentiable extension in a neighborhood of $[-1, 1]$, we prefer to simply introduce the following definition.

Definition 1 Suppose that $f : [-1, 1] \rightarrow \mathbb{C}$ admits an infinitely differentiable extension to an open interval containing $[-1, 1]$. Then, for each real number $0 < \epsilon < 1$, we denote by $c_f(\epsilon)$ the smallest positive real number c such that there exists a function $f_b \in S(\mathbb{R})$ of bandlimit c with the following properties:

1. $\|f - f_b\|_{L^\infty([-1, 1])} \leq \epsilon \|f\|_{L^\infty([-1, 1])}$,
2. $\|f_b\|_{L^\infty(\mathbb{R})} \leq 4 \|f\|_{L^\infty([-1, 1])}$,
3. $\|\widehat{f}_b\|_{L^\infty(\mathbb{R})} \leq 4 \|f\|_{L^\infty([-1, 1])}$ and
4. $\|\widehat{f}_b'\|_{L^\infty(\mathbb{R})} \leq 4 \|f\|_{L^\infty([-1, 1])}$.

The following is an immediate consequence of Theorem 1.

Corollary 1 *If $f : [-1, 1] \rightarrow \mathbb{C}$ admits an infinitely differentiable extension to a neighborhood of $[-1, 1]$, then for every positive integer m ,*

$$c_f(\epsilon) = \mathcal{O} \left(\left(\frac{1}{\epsilon} \right)^{\frac{1}{m}} \right) \quad \text{as } \epsilon \rightarrow 0. \quad (41)$$

Under the assumption that $f : [-1, 1] \rightarrow \mathbb{C}$ admits an extension which is bounded and analytic on a horizontal strip containing the real axis, then we clearly have

$$c_f(\epsilon) = \mathcal{O} \left(\log \left(\frac{1}{\epsilon} \right) \right) \quad \text{as } \epsilon \rightarrow 0. \quad (42)$$

We conjecture that this also holds when f admits an extension which is analytic in an open neighborhood of $[-1, 1]$, but a proof of this is beyond the scope of the present article.

2.4 Legendre expansions of bandlimited functions

It is a consequence of the Schwartz-Paley-Wiener theorem that if $\widehat{\varphi}$ has compact support, then φ is an entire function satisfying certain growth conditions at ∞ . It follows from this and standard results in approximation theory (which can be found in [18], for example) that the Legendre expansion of φ decays superexponentially. Here, for the sake of concreteness, we give a simple bound on the coefficients in the Legendre expansion of φ which depends on the order n of $\widehat{\varphi}$ and its bandlimit c . Throughout this subsection, we use P_k to denote the Legendre polynomial of degree k and j_ν to denote the spherical Bessel function of order ν . Definitions of these functions can be found, for instance, in [19].

Lemma 1 *If φ is a tempered distribution of order n which is supported on $[a, b]$, then there exist complex numbers c_0, \dots, c_{n-1} and a complex Radon measure μ on $[a, b]$ such that*

$$\langle \varphi, f \rangle = \sum_{k=0}^{n-1} c_k f^{(k)}(a) + \int_a^b f(x) d\mu(x). \quad (43)$$

for all $f \in C^n([a, b])$.

Proof Because the space of tempered distributions of order n which are supported on $[a, b]$ can be identified with the dual space of $C^n([a, b])$, it suffices to show that any element of the dual of $C^n([a, b])$ is of the form (43). The case $n = 0$ follows by a trivial application of the Riesz representation theorem, so we suppose that $n \geq 1$. Because any function $f \in C^n([a, b])$ can be written as

$$f(x) = \sum_{k=0}^{n-1} \frac{f^{(k)}(a)}{k!} (x-a)^k + \int_a^x \frac{f^{(n)}(u)}{(n-1)!} (u-a)^{n-1} du, \quad (44)$$

the map

$$f \mapsto \left(f(a), f'(a), \dots, f^{(n-1)}(a), f^{(n)} \right) \quad (45)$$

is an isomorphism from $C^n([a, b])$ to $\mathbb{C}^n \times C([a, b])$. The result now follows from this and the observations that the dual of $C([a, b])$ is the space of complex Radon measures $M([a, b])$ and \mathbb{C}^n is its own dual space. \square

Lemma 2 *If the Fourier transform of the tempered distribution φ is of order n and has support on the interval $[a, b]$, then φ coincides with an entire function of the form*

$$\varphi(x) = p_{n-1}(x) + x^n \int_a^b e^{i\xi x} d\mu(\xi), \quad (46)$$

where p_{n-1} is a polynomial of degree at most $n-1$ and $\mu \in M([a, b])$.

12 *On the adaptive Levin method*

Proof The tempered distribution φ is given by

$$\varphi(x) = \langle \widehat{\varphi}, \xi_x \rangle, \quad (47)$$

where $\xi_x(\xi) = \exp(ix\xi)$. The result follows from this and Lemma 1. \square

Lemma 3 *For all real-valued ξ and nonnegative integers k ,*

$$\left| \int_{-1}^1 \exp(i\xi x) P_k(x) dx \right| \leq \frac{2 \left| \frac{\xi}{2} \right|^k}{\Gamma(k+1)}. \quad (48)$$

Proof The formula

$$\int_{-1}^1 \exp(i\xi x) P_k(x) dx = 2i^k j_k(\xi), \quad (49)$$

can be found in Section 7.8 of [20], among many other sources. Combining it with the well-known inequality

$$|j_k(z)| \leq \frac{\left| \frac{z}{2} \right|^k}{\Gamma(k+1)}, \quad (50)$$

which is a special case of Formula 10.14.4 in [19], yields the conclusion of the lemma. \square

Theorem 2 *Suppose that the Fourier transform of $\varphi \in S'(\mathbb{R})$ is a tempered distribution of order n supported on the interval $[-c, c]$ with $c \geq 1$. Then φ is an entire function and the coefficients in the Legendre expansion*

$$\varphi(x) = \sum_{m=0}^{\infty} a_m P_m(x) \quad (51)$$

of φ satisfy

$$|a_m| \lesssim \frac{\left(\frac{c}{2}\right)^{m+n}}{\Gamma(m-n+1)}. \quad (52)$$

for all $m \geq n$.

Proof By Lemma 2,

$$\begin{aligned} \int_{-1}^1 \varphi(x) P_m(x) dx &= \int_{-1}^1 p_{n-1}(x) P_m(x) dx \\ &\quad + \int_{-c}^c \left(\int_{-1}^1 x^n \exp(i\xi x) P_m(x) dx \right) d\mu(\xi), \end{aligned} \quad (53)$$

where p_{n-1} is a polynomial of degree at most $n-1$ and $\mu \in M([-c, c])$. For $m \geq n$,

$$\int_{-1}^1 p_{n-1}(x) P_m(x) dx = 0, \quad (54)$$

and so

$$\left| \int_{-1}^1 \varphi(x) P_m(x) dx \right| \leq |\mu| ([-c, c]) \max_{\xi \in [-c, c]} \left| \int_{-1}^1 \exp(i\xi x) x^n P_m(x) dx \right|. \quad (55)$$

We now observe that

$$x^n P_m(x) = \sum_{k=m-n}^{m+n} b_k P_k(x), \quad (56)$$

where

$$b_k = \sqrt{k + \frac{1}{2}} \int_{-1}^1 x^n P_m(x) P_k(x) dx. \quad (57)$$

By combining (56) and Lemma 3, we see that

$$\begin{aligned} \left| \int_{-1}^1 \exp(i\xi x) x^n P_m(x) dx \right| &\leq \sum_{k=m-n}^{m+n} \frac{2|b_k| \left| \frac{\xi}{2} \right|^k}{\Gamma(k+1)} \\ &\leq \frac{(4n+2) \max\{|b_k|\} \left(\frac{c}{2} \right)^{m+n}}{\Gamma(m-n+1)}, \end{aligned} \quad (58)$$

for all $|\xi| \leq c$. Together with (55), this gives us (52). \square

Remark 1. Using the well-known approximation

$$j_\nu(z) \approx \frac{1}{z\sqrt{2e}} \left(\frac{ez}{2(\nu + \frac{1}{2})} \right)^{\nu+1} = \left(\frac{e}{2\sqrt{2e}(\nu + \frac{1}{2})} \right) \left(\frac{ez}{2(\nu + \frac{1}{2})} \right)^\nu \quad (59)$$

in lieu of the rather crude bound (50), we see that

$$\begin{aligned} &\left| \int_{-1}^1 \exp(i\xi x) x^n P_m(x) dx \right| \\ &= \left| \sum_{k=m-n}^{m+n} 2i^k b_k j_k(\xi) \right| \\ &\leq (4n+2) \max\{|b_k|\} \sum_{k=m-n}^{m+n} |j_k(\xi)| \\ &\approx (4n+2) \max\{|b_k|\} \sum_{k=m-n}^{m+n} \left(\frac{e}{2\sqrt{2e}(k + \frac{1}{2})} \right) \left(\frac{ec}{2(k + \frac{1}{2})} \right)^k \end{aligned} \quad (60)$$

for all $|\xi| \leq c$. When $m > ec/2 + n - \frac{1}{2}$,

$$\left(\frac{ec}{2(k + \frac{1}{2})} \right) < 1 \quad (61)$$

and the preceding sum is bounded by a multiple of

$$\frac{2n}{m-n + \frac{1}{2}} \left(\frac{ec}{2(m-n + \frac{1}{2})} \right)^{m-n}. \quad (62)$$

So we expect the coefficients in the Legendre expansion of φ to decay superexponentially as soon as this condition is met.

2.5 Truncated singular value decompositions

If \mathcal{A} is a complex-valued $n \times n$ matrix, then any decomposition of the form

$$\mathcal{A} = \begin{pmatrix} \overline{u_1} & \overline{u_2} & \cdots & \overline{u_n} \end{pmatrix} \begin{pmatrix} \sigma_1 & & & \\ & \sigma_2 & & \\ & & \ddots & \\ & & & \sigma_n \end{pmatrix} \begin{pmatrix} \overline{v_1} & \overline{v_2} & \cdots & \overline{v_n} \end{pmatrix}^*, \quad (63)$$

where $\sigma_1, \dots, \sigma_n \in \mathbb{R}$ and both $\{\overline{u_1}, \dots, \overline{u_n}\}$ and $\{\overline{v_1}, \dots, \overline{v_n}\}$ are orthonormal bases in \mathbb{C}^n , is known as a singular value decomposition of \mathcal{A} . The quantities $\sigma_1, \dots, \sigma_n$ are uniquely determined up to ordering, and they are known as the singular values of \mathcal{A} . It is conventional to arrange them in descending order, and we will assume that this is the case with all singular value decompositions that we consider.

A truncated singular value decomposition of \mathcal{A} is any approximation of the form

$$\mathcal{A} \approx \begin{pmatrix} \overline{u_1} & \overline{u_2} & \cdots & \overline{u_k} \end{pmatrix} \begin{pmatrix} \sigma_1 & & & \\ & \sigma_2 & & \\ & & \ddots & \\ & & & \sigma_k \end{pmatrix} \begin{pmatrix} \overline{v_1} & \overline{v_2} & \cdots & \overline{v_k} \end{pmatrix}^*, \quad (64)$$

where (63) is a singular value decomposition of A and $1 \leq k \leq n$. Typically, some desired precision $\epsilon > 0$ is specified and k is taken to be the least integer between 1 and $n - 1$ such that $\sigma_{k+1} < \epsilon$, if such an integer exists, or $k = n$ otherwise. We say that (64) is a singular value decomposition which has been truncated at precision ϵ when k has been chosen in this fashion. We call the vector

$$\overline{x} = \begin{pmatrix} \overline{v_1} & \overline{v_2} & \cdots & \overline{v_k} \end{pmatrix} \begin{pmatrix} \frac{1}{\sigma_1} & & & \\ & \frac{1}{\sigma_2} & & \\ & & \ddots & \\ & & & \frac{1}{\sigma_k} \end{pmatrix} \begin{pmatrix} \overline{u_1} & \overline{u_2} & \cdots & \overline{u_k} \end{pmatrix}^* y \quad (65)$$

the solution of the linear system $Ax = y$ obtained from the truncated singular value decomposition (64).

The following theorem implies that, when a linear system admits an approximate solution with a modest norm, and it is solved numerically using a truncated singular value decomposition, the computed solution will have both a small residual and a modest norm. The proof can be found in [21].

Theorem 3 Suppose that $\mathcal{A} \in \mathbb{R}^{m \times n}$, where $m \geq n$, and let $\sigma_1 \geq \sigma_2 \geq \dots \geq \sigma_n$ be the singular values of \mathcal{A} . Suppose that $\bar{x} \in \mathbb{R}^n$ satisfies

$$\mathcal{A}\bar{x} = \bar{b}. \quad (66)$$

Let $\epsilon > 0$, and suppose that

$$\hat{x}_k = (\mathcal{A} + \mathcal{E})_k^\dagger (\bar{b} + \bar{e}), \quad (67)$$

where $(\mathcal{A} + \mathcal{E})_k^\dagger$ is the pseudo-inverse of the k -TSVD of $\mathcal{A} + \mathcal{E}$, so that

$$\hat{\sigma}_k \geq \epsilon \geq \hat{\sigma}_{k+1}, \quad (68)$$

where $\hat{\sigma}_k$ and $\hat{\sigma}_{k+1}$ are the k th and $(k+1)$ th largest singular values of $\mathcal{A} + \mathcal{E}$, and where $\mathcal{E} \in \mathbb{R}^{m \times n}$ and $\bar{e} \in \mathbb{R}^m$, with $\|\mathcal{E}\|_2 < \epsilon/2$. Then

$$\|\hat{x}_k\|_2 \leq \frac{1}{\hat{\sigma}_k} (2\epsilon \|\bar{x}\|_2 + \|\bar{e}\|_2) + \|\bar{x}\|_2. \quad (69)$$

and

$$\|\mathcal{A}\hat{x}_k - \bar{b}\|_2 \leq 5\epsilon \|\bar{x}\|_2 + \frac{3}{2} \|\bar{e}\|_2. \quad (70)$$

We will make use of the following simplified version of this theorem.

Corollary 2 Suppose that $\epsilon > 0$, \mathcal{A} is an $n \times n$ matrix with complex entries, and that

$$\mathcal{A}\bar{x} = \bar{y} + \bar{\delta y} \quad (71)$$

for some \bar{x} , \bar{y} and $\bar{\delta y}$ in \mathbb{C}^n with

$$\|\bar{\delta y}\| \lesssim \epsilon \|\mathcal{A}\| \|\bar{x}\|. \quad (72)$$

Suppose further that the linear system

$$\mathcal{A}\bar{x} = \bar{y} \quad (73)$$

is solved in finite precision arithmetic using a singular value decomposition which is truncated at precision $\epsilon \|\mathcal{A}\|$, and that \bar{z} is the computed solution. Then

$$\|\bar{z}\| \lesssim \|\bar{x}\| \quad (74)$$

and

$$\|\mathcal{A}\bar{z} - \bar{y}\| \lesssim \epsilon \|\mathcal{A}\| \|\bar{x}\|. \quad (75)$$

3 Analysis of the Levin equation

This section contains our analysis of the Levin equation. The two principal results are Theorems 4 and 5. Theorem 4 generalizes the classical result of [1] by showing that, whenever g' is nonzero over the interval and the ratio of the maximum value of g' to the minimum value of g' is small, the Levin equation admits a well-behaved solution which can be approximated by a polynomial expansion at a cost which is independent of the magnitude of g' . Theorem 5 shows that, on an interval in which g' is of small magnitude, the Levin equation admits a well-behaved solution which can be represented by a

polynomial expansion at a cost which decreases with the magnitude of g' . It applies whether or not g' has zeros in the interval. Throughout, we use the “ \lesssim notation” to suppress constants which do not depend on the magnitude of g' . We begin with the following lemma, which applies in the simple case when g' is a nonzero constant.

Lemma 4 *Suppose that $f : [-1, 1] \rightarrow \mathbb{C}$ admits an infinitely differentiable extension to a neighborhood of $[-1, 1]$ and $W \neq 0$. Then for each $0 < \epsilon < 1$, there exists a function $p_b \in S(\mathbb{R})$ such that*

1. \widehat{p}_b is a tempered distribution of order one supported on $[-c_f(\epsilon), c_f(\epsilon)]$,
2. $|p'_b(x) + iWp_b(x)| \leq \epsilon \|f\|_{L^\infty([-1,1])}$ for all $x \in [-1, 1]$,
3. $\|p_b\|_{L^\infty([-1,1])} \lesssim \min \left\{ 1, \frac{1}{|W|} \right\} \|f\|_{L^\infty([-1,1])}$ and
4. $\|p'_b\|_{L^\infty([-1,1])} \lesssim \min \left\{ 1, \frac{1}{|W|} \right\} \|f\|_{L^\infty([-1,1])}$.

Proof We let $f_b \in S(\mathbb{R})$ be a function with bandlimit $W_0 = c_f(\epsilon)$ such that conditions (1)-(5) in Definition 1 hold, and define the function p_b via the formula

$$p_b(x) = \text{p.v.} \int_{-W_0}^{W_0} \frac{\widehat{f}_b(\xi)}{i(W + \xi)} \exp(i\xi x) d\xi. \quad (76)$$

That is, p_b is the inverse Fourier transform of the product of the tempered distribution T defined via

$$\langle T, \varphi \rangle = \text{p.v.} \int_{-\infty}^{\infty} \frac{\varphi(\xi)}{i(W + \xi)} d\xi \quad (77)$$

and the infinitely differentiable function \widehat{f}_b . It is clear that \widehat{p}_b is a tempered distribution of order one which is supported on $[-W_0, W_0]$, so the first of the conditions listed above is satisfied.

Since

$$p'_b(x) + iWp_b(x) = \int_{-W_0}^{W_0} \frac{i(W + \xi) \widehat{f}_b(\xi)}{i(W + \xi)} \exp(i\xi x) d\xi = f_b(x) \quad (78)$$

and

$$\|f - f_b\|_{L^\infty([-1,1])} \leq \epsilon \|f\|_{L^\infty([-1,1])}, \quad (79)$$

the second of the properties of p_b listed above holds.

To establish the third of the properties of p_b listed above, we first assume that $|W| \leq W_0 + 1$. Then we have

$$\begin{aligned} p_b(x) &= \text{p.v.} \int_{-W_0}^{W_0} \frac{\widehat{f}_b(\xi)}{i(W + \xi)} \exp(i\xi x) d\xi \\ &= \text{p.v.} \int_{-W-2W_0-1}^{-W+2W_0+1} \frac{\widehat{f}_b(\xi)}{i(W + \xi)} \exp(i\xi x) d\xi \\ &= \int_{-W-2W_0-1}^{-W+2W_0+1} \frac{\widehat{f}_b(\xi) \exp(i\xi x) - \widehat{f}_b(-W) \exp(-ixW)}{i(W + \xi)} d\xi \end{aligned} \quad (80)$$

for all $x \in \mathbb{R}$, where the last equality follows from the fact that $1/(W + \xi)$ is odd about $\xi = -W$. By the mean value theorem, there exists a function $\eta(\xi)$ such that

$$p_b(x) = \int_{-W-2W_0-1}^{-W+2W_0+1} \frac{G'(\eta(\xi))(W + \xi)}{i(W + \xi)} d\xi = -i \int_{-W-2W_0-1}^{-W+2W_0+1} G'(\eta(\xi)) d\xi \quad (81)$$

for all $x \in \mathbb{R}$, where

$$G(\xi) = \widehat{f}_b(\xi) \exp(ix\xi). \quad (82)$$

Since

$$G'(\xi) = \widehat{f}_b'(\xi) \exp(ix\xi) + ix\widehat{f}_b(\xi) \exp(ix\xi), \quad (83)$$

we have

$$|p_b(x)| \leq 2(2W_0 + 1) \left(\|\widehat{f}_b'\|_{L^\infty(\mathbb{R})} + \|\widehat{f}_b\|_{L^\infty(\mathbb{R})} \right) \quad (84)$$

for all $x \in [-1, 1]$ (note that we are now only considering x in $[-1, 1]$). Now making use of properties (4) and (5) in Definition 1 gives us

$$\|p_b\|_{L^\infty([-1,1])} \leq 16(2W_0 + 1) \|f\|_{L^\infty([-1,1])}. \quad (85)$$

An analogous argument which makes use of the fact that

$$p_b'(x) = \int_{-W-2W_0-1}^{-W+2W_0+1} \frac{H(\xi) - H(-W)}{i(W + \xi)} d\xi, \quad (86)$$

where

$$H(\xi) = i\xi\widehat{f}_b(\xi) \exp(ix\xi), \quad (87)$$

shows that

$$\begin{aligned} \|p_b'\|_{L^\infty([-1,1])} &\leq 8(2W_0 + 1) (1 + 2(|W| + 2W_0 + 1)) \|f\|_{L^\infty([-1,1])} \\ &\leq 8(2W_0 + 1) (6W_0 + 5) \|f\|_{L^\infty([-1,1])} \end{aligned} \quad (88)$$

when $|W| \leq W_0 + 1$.

We now suppose that $|W| > W_0 + 1$. Then

$$|p_b(x)| = \left| \int_{-W_0}^{W_0} \frac{\widehat{f}_b(\xi) \exp(i\xi x)}{i(W + \xi)} d\xi \right| \leq \frac{2W_0}{|W| - |W_0|} \|\widehat{f}_b\|_{L^1(\mathbb{R})} \quad (89)$$

and

$$|p_b'(x)| = \left| \int_{-W_0}^{W_0} \frac{\widehat{f}_b(\xi) \exp(i\xi x) i\xi}{i(W + \xi)} d\xi \right| \leq \frac{2W_0^2}{|W| - |W_0|} \|\widehat{f}_b\|_{L^1(\mathbb{R})} \quad (90)$$

hold for all $x \in \mathbb{R}$. From the above inequalities, the fact that

$$\frac{1}{|W| - W_0} \leq \frac{W_0 + 1}{|W|} \quad (91)$$

and property (4) in Definition 1, we see that

$$\|p_b\|_{L^\infty(\mathbb{R})} \leq \frac{8W_0(W_0 + 1)}{|W|} \|f\|_{L^\infty([-1,1])} \quad (92)$$

and

$$\|p_b'\|_{L^\infty(\mathbb{R})} \leq \frac{8W_0^2(W_0 + 1)}{|W|} \|f\|_{L^\infty([-1,1])} \quad (93)$$

whenever $|W| > W_0 + 1$. The third of the conditions on p_b listed in the conclusion of the lemma follows from the combination of (85) and (92), while the fourth is obtained by combining (88) and (93). \square

In accordance with Remark 1, the sequence $\{a_m\}$ of Legendre coefficients of the approximate solution p_b of Levin's equation appearing in Lemma 4 decays superexponentially once $m > e/2c_f(\epsilon) + 1/2$. Consequently, p_b can be represented to a fixed relative precision via a polynomial expansion at a cost which depends on the complexity of f but not the magnitude of W .

We now move on to the case in which g' is nonconstant, but with no zeros on the interval $[-1, 1]$. To that end, we suppose that $f : [-1, 1] \rightarrow \mathbb{C}$ and $g : [-1, 1] \rightarrow \mathbb{R}$ admit infinitely differentiable extensions to a neighborhood of $[-1, 1]$, and that the extension of g' is nonzero in an open interval containing $[-1, 1]$. We also let

$$G_0 = \min_{-1 \leq x \leq 1} |g'(x)|, \quad W = \frac{1}{2} \int_{-1}^1 g'(x) dx \quad (94)$$

and define $u : [-1, 1] \rightarrow [-1, 1]$ via the formula

$$u(x) = -1 + \frac{1}{W} \int_{-1}^x g'(y) dy. \quad (95)$$

Because g' is nonzero in a neighborhood of $[-1, 1]$, u is invertible and its inverse extends to an open neighborhood of $[-1, 1]$. Finally, we define $h : [-1, 1] \rightarrow [-1, 1]$ via the formula

$$h(z) = \frac{f(u^{-1}(z))}{u'(u^{-1}(z))} = f(u^{-1}(z)) \frac{du^{-1}}{dz}(z). \quad (96)$$

With the preceding notations and assumptions, we have the following:

Theorem 4 *For every $0 < \epsilon < 1$, there exists a function $p_b : [-1, 1] \rightarrow \mathbb{C}$ such that*

1. *the Fourier transform of $p_b(u^{-1}(z))$ is a tempered distribution of order 1 supported on the interval $[-c_h(\epsilon), c_h(\epsilon)]$,*
2. *$|p'_b(x) + ig'(x)p_b(x) - f(x)| \leq \epsilon \frac{|W|}{G_0} \|f\|_{L^\infty([-1, 1])}$ for all $x \in [-1, 1]$,*
3. *$\|p_b\|_{L^\infty([-1, 1])} \lesssim \frac{|W|}{G_0} \min \left\{ 1, \frac{1}{|W|} \right\} \|f\|_{L^\infty([-1, 1])}$ and*
4. *$\|p'_b\|_{L^\infty([-1, 1])} \lesssim \frac{|W|}{G_0} \min \left\{ 1, \frac{1}{|W|} \right\} \|f\|_{L^\infty([-1, 1])}$.*

Proof By introducing the new variable $z = u(x)$, we transform the Levin equation

$$p'(x) + ig'(x)p(x) = f(x), \quad -1 < x < 1, \quad (97)$$

into the simplified form

$$p'(z) + iWp(z) = h(z), \quad -1 < z < 1. \quad (98)$$

Our assumptions on f and g , and the method we used to construct u ensure that h admits an infinitely differentiable extension to a neighborhood of $[-1, 1]$. Applying Lemma 4 to (98) shows that, for all $0 < \epsilon < 1$, there exists an entire function p_1 such that

1. \widehat{p}_1 is a tempered distribution of order 1 supported on the interval $[-c_h(\epsilon), c_h(\epsilon)]$,
2. $|p'_1(z) + iWp_1(z) - h(z)| \leq \epsilon \|h\|_{L^\infty([-1,1])}$ for all $z \in [-1, 1]$,
3. $\|p_1\|_{L^\infty([-1,1])} \lesssim \min \left\{ 1, \frac{1}{|W|} \right\} \|h\|_{L^\infty([-1,1])}$ and
4. $\|p'_1\|_{L^\infty([-1,1])} \lesssim \min \left\{ 1, \frac{1}{|W|} \right\} \|h\|_{L^\infty([-1,1])}$.

We now define p_b via the formula $p_b(x) = p_1(u(x))$. It is clear that the first condition on p_b listed above is satisfied. We observe that, since $g'(x) = Wu'(x)$,

$$\|h\|_{L^\infty([-1,1])} \leq \frac{|W|}{G_0} \|f\|_{L^\infty([-1,1])}. \quad (99)$$

Combining (99) and properties of p_1 listed above yields

$$\|p_b\|_{L^\infty([-1,1])} \lesssim \frac{|W|}{G_0} \min \left\{ 1, \frac{1}{|W|} \right\} \|f\|_{L^\infty([-1,1])}, \quad (100)$$

$$\|p'_b\|_{L^\infty([-1,1])} \lesssim \frac{|W|}{G_0} \min \left\{ 1, \frac{1}{|W|} \right\} \|f\|_{L^\infty([-1,1])} \quad (101)$$

and

$$|p_b(x) - ig'(x)p_b(x) - f(x)| \leq \epsilon \frac{|W|}{G_0} \|f\|_{L^\infty([-1,1])}, \quad (102)$$

the latter of which holds for all $x \in [-1, 1]$. This suffices to establish the theorem. \square

We emphasize that Theorem 4 does not imply that the approximate solution p_b of the Levin equation has a Fourier transform which is a tempered distribution with compact support. Instead, we have

$$p_b(x) = \langle \widehat{p}_1, \eta_x \rangle \quad \text{with} \quad \eta_x(\xi) = \exp(iu(x)\xi), \quad (103)$$

where \widehat{p}_1 is a tempered distribution of order one with compact support (c.f., Formula (A3) in the original Levin paper [1]). Since p_b is the composition of the entire function p_1 and the function u , which is infinitely differentiable on a neighborhood of $[-1, 1]$, the magnitudes of the coefficients $\{a_m\}$ in its Legendre expansion decay faster than m^{-k} for any positive integer k . Moreover, (103) implies that p_b can be approximated to a fixed relative precision via a Legendre expansion at a cost which depends on the complexity of f and g^{-1} , but not on the magnitude of g' . To see this, we first note that h is defined in terms of f and the normalized version u of g , so that $c_h(\epsilon)$ does not depend on the magnitude of g' . The bandlimit of p_1 then depends on $c_h(\epsilon)$, and p_b is obtained by the composition of p_1 with the normalized version u of g .

It would be of interest to develop better estimates on the rate of decay of the Legendre coefficients of p_b , as we did in the case when g' is constant, but useful results of this type seem to be fairly complicated. Indeed, the difficulty in estimating the complexity of p_b *a priori* is one of the principal motivations for the adaptive version of the Levin algorithm that we introduce in this article.

We close this section with the following theorem which shows that, if g' is of small magnitude, then the Levin equation admits a solution which can be well-approximated by a bounded, bandlimited function p_b .

Theorem 5 *Suppose that $f : [-1, 1] \rightarrow \mathbb{C}$ and $g : [-1, 1] \rightarrow \mathbb{R}$ admit extensions to infinitely differentiable functions in a neighborhood of $[-1, 1]$, and that*

$$G_1 = \max_{-1 \leq x \leq 1} |g'(x)| < \frac{1}{2}. \quad (104)$$

Let $0 < \epsilon < 1$ be given, and define the integer n via the formula

$$n = \left\lfloor \frac{\log(\epsilon)}{\log(2G_1)} \right\rfloor. \quad (105)$$

Then there exists $p_b \in C^\infty(\mathbb{R})$ such that

1. \widehat{p}_b is a tempered distribution of order 1 supported on the interval

$$[-c_f(\epsilon) - nc_{g'}(\epsilon), c_f(\epsilon) + nc_{g'}(\epsilon)], \quad (106)$$

2. $|p'_b(x) + ig'(x)p_b(x) - f(x)| \leq 2\epsilon \left(1 + \frac{G_1}{1 - 2G_1}\right) \|f\|_{L^\infty([-1, 1])}$ for all $x \in [-1, 1]$,

3. $\|p_b\|_{L^\infty([-1, 1])} \leq \frac{2}{1 - 2G_1} \|f\|_{L^\infty([-1, 1])}$ and

4. $\|p'_b\|_{L^\infty([-1, 1])} \leq 4 \left(1 + \frac{G_1}{1 - 2G_1}\right) \|f\|_{L^\infty([-1, 1])}.$

Proof We let f_b and g'_b be bandlimited approximates of f and g' which satisfy conditions (1)-(5) in Definition 1. We next define $A : L^\infty([-1, 1]) \rightarrow L^\infty([-1, 1])$ via the formula

$$A[\varphi](x) = -i \int_0^x g'_b(y) \varphi(y) dy. \quad (107)$$

Obviously, $\|A\|_\infty$ is bounded by $\|g'_b\|_{L^\infty([-1, 1])}$, which is less than $(1 + \epsilon)G_1 \leq 2G_1 < 1$ by property (1) in Definition 1. Now we let $G_2 = (1 + \epsilon)G_1$,

$$h(x) = \int_0^x f_b(y) dy \quad (108)$$

and

$$p_b(x) = \sum_{k=0}^n A^k[h](x), \quad (109)$$

where A^k denotes the repeated application of the operator A and n is defined by (105). Since $\|f_b\|_{L^\infty([-1,1])} \leq (1+\epsilon)\|f\|_{L^\infty([-1,1])}$ by property (1) of Definition 1, we have

$$\begin{aligned} \|p_b\|_{L^\infty([-1,1])} &\leq \left(\sum_{k=0}^n \|A\|_\infty^k \right) \|h\|_{L^\infty([-1,1])} \\ &\leq \frac{1 + G_2^{n+1}}{1 - G_2} \|f\|_{L^\infty([-1,1])} \\ &\leq \frac{1 + \epsilon}{1 - G_2} \|f\|_{L^\infty([-1,1])}, \end{aligned} \quad (110)$$

which implies the third property of p_b listed above. Since $h'(x) = f_b(x)$ and

$$\frac{d}{dx} A^k [h](x) = -ig'_b(x) A^{k-1} [h](x), \quad (111)$$

we have

$$\begin{aligned} p'_b(x) &= f_b(x) - ig'_b(x) \sum_{k=0}^{n-1} A^k [h](x) \\ &= f_b(x) - ig'_b(x) \sum_{k=0}^n A^k [h](x) + ig'_b(x) A^n [h](x) \\ &= f_b(x) - ig'_b(x) p_b(x) + ig'_b(x) A^n [h](x) \end{aligned} \quad (112)$$

for all $x \in [-1, 1]$. From this and (110), we see that

$$\begin{aligned} \|p'_b(x)\|_{L^\infty([-1,1])} &\leq \|f_b\|_{L^\infty([-1,1])} + \|g'\|_{L^\infty([-1,1])} \|p_b\|_{L^\infty([-1,1])} \\ &\quad + G_2^{n+1} \|f_b\|_{L^\infty([-1,1])} \\ &\leq \left((1+\epsilon) + G_1 \frac{1+\epsilon}{1-G_2} + \epsilon(1+\epsilon) \right) \|f\|_{L^\infty([-1,1])} \\ &\leq \left((1+\epsilon)^2 + \frac{2G_1}{1-G_2} \right) \|f\|_{L^\infty([-1,1])}, \end{aligned} \quad (113)$$

from which the fourth of the properties of p_b listed in the conclusion of the theorem follows. Similarly, (112) implies that

$$\begin{aligned} |p'_b(x) + ig'_b(x) p_b(x) - f(x)| &\leq |p'_b(x) + ig'_b(x) p_b(x) - f_b(x)| + |f_b(x) - f(x)| \\ &\leq |ig'_b(x) A^n [h](x)| + |f_b(x) - f(x)| \\ &\leq G_2^{n+1} \|f\|_{L^\infty([-1,1])} + \epsilon \|f\|_{L^\infty([-1,1])} \\ &\leq 2\epsilon \|f\|_{L^\infty([-1,1])} \end{aligned} \quad (114)$$

for all $x \in [-1, 1]$. Combining (114) with (110), (113) and using the properties of the approximates f_b and g_b , we see that

$$\begin{aligned} &|p'_b(x) + ig'(x) p_b(x) - f(x)| \\ &\leq |p'_b(x) + ig'_b(x) p_b(x) - f(x)| + |ig'(x) p_b(x) - ig'_b(x) p_b(x)| \\ &\leq 2\epsilon \|f\|_{L^\infty([-1,1])} + \|p_b\|_{L^\infty([-1,1])} \|g' - g'_b\|_{L^\infty([-1,1])} \\ &\leq \left(2 + \left(\frac{1+\epsilon}{1-G_2} \right) \left(\|g'\|_{L^\infty([-1,1])} \right) \right) \epsilon \|f\|_{L^\infty([-1,1])} \end{aligned} \quad (115)$$

for all $x \in [-1, 1]$. The second of the properties of p_b listed above follows from (115).

It remains only to establish the first of the properties of p_b listed above. To do so, we first observe that the Fourier transform of h is

$$\text{p.v.} \frac{\widehat{f_b}(\xi)}{i\xi} + \frac{1}{2}\delta(\xi) \left(\int_0^\infty f_b(x) dx - \int_{-\infty}^0 f_b(x) dx \right), \quad (116)$$

which is a tempered distribution of order one supported on the interval $[-c_\epsilon(f), c_\epsilon(f)]$. Next, we suppose that ψ is a $C^\infty(\mathbb{R})$ function whose Fourier transform is a tempered distribution of order 1 supported on $[-c, c]$. The Fourier transform of the convolution of ψ with the function $g'_b \in S(\mathbb{R})$ is a tempered distribution of order 0 supported on $[-c - c_{g'}, c + c_{g'}]$. Since $A[\psi]$ is obtained by integrating this convolution, its Fourier transform is a tempered distribution of order 1 with bandlimit $[-c - c_{g'}(\epsilon), c + c_{g'}(\epsilon)]$. It now follows by induction that the Fourier transform of $A^k[h]$ is a tempered distribution of order 1 with bandlimit $[-c_f(\epsilon) - kc_{g'}(\epsilon), c_f(\epsilon) + kc_{g'}(\epsilon)]$. Combining this with (109) yields the first property of p_b listed above. \square

The bandlimit of the function p_b whose existence is established in Theorem 5 decreases with magnitude of g' . Consequently, on any interval on which g' is sufficiently small, we expect to be able to represent p_b to a fixed relative accuracy with a polynomial expansion whose number of terms is bounded. Moreover, this is the case whether or not g' has zeros in the interval.

4 Numerical aspects of the Levin method

In this section, we show that high-accuracy can be obtained when the Levin equation (2) is discretized via a Chebyshev spectral collocation method and the resulting linear system is solved with a truncated singular value decomposition, regardless of the magnitude of g' and whether or not it has zeros. To that end, we suppose that $f : [-1, 1] \rightarrow \mathbb{C}$ and $g : [-1, 1] \rightarrow \mathbb{R}$ admit continuously differentiable extensions to a neighborhood of $[-1, 1]$, and that $0 < \epsilon < 1$. Moreover, we let

$$G_0 = \min_{-1 \leq x \leq 1} |g'(x)|, \quad G_1 = \max_{-1 \leq x \leq 1} |g'(x)| \quad \text{and} \quad W = \frac{1}{2} \int_{-1}^1 g'(x) dx. \quad (117)$$

We first consider the case in which $G_0 > 0$ and invoke Theorem 4 to see that there exists a bandlimited function p_b such that

$$|p'_b(x) + ig'(x)p_b(x) - f(x)| \leq \epsilon \frac{|W|}{G_0} \|f\|_{L^\infty([-1,1])} \quad \text{for all } x \in [-1, 1], \quad (118)$$

$$\|p_b\|_{L^\infty([-1,1])} \lesssim \frac{|W|}{G_0} \min \left\{ 1, \frac{1}{|W|} \right\} \|f\|_{L^\infty([-1,1])} \quad (119)$$

and

$$\|p'_b\|_{L^\infty([-1,1])} \lesssim \frac{|W|}{G_0} \min \left\{ 1, \frac{1}{|W|} \right\} \|f\|_{L^\infty([-1,1])}. \quad (120)$$

Moreover, it is clear from the discussion following Theorem 4 that

$$p_b(x) = \sum_{n=0}^{\infty} a_n T_n(x), \quad (121)$$

where $|a_n|$ is bounded by a rapidly decaying function of n which is independent of the magnitude of g' .

We claim that there is an integer k such that

$$\begin{aligned} & \left\| \mathbf{P}_k[p_b]' + i\mathbf{P}_k[g']\mathbf{P}_k[p_b] - (p_b' + ig'p_b) \right\|_{L^\infty([-1,1])} \\ & \leq \epsilon \|p_b'\|_{L^\infty([-1,1])} + 4\epsilon G_1 \|p_b\|_{L^\infty([-1,1])} \\ & \lesssim \epsilon (1 + 4G_1) \frac{|W|}{G_0} \min \left\{ 1, \frac{1}{|W|} \right\} \|f\|_{L^\infty([-1,1])} \end{aligned} \quad (122)$$

holds regardless of the values of $|W|$ and G_1 ; that is, k can be chosen independent of the magnitude of g' . To see this, we first observe that (121) together with Formulas (28) and (29) in Subsection 2.2 imply that we can choose k independently of G_1 and $|W|$ such that

$$\|\mathbf{P}_k[p_b] - p_b\|_{L^\infty([-1,1])} \leq \epsilon \|p_b\|_{L^\infty([-1,1])} \quad (123)$$

and

$$\|\mathbf{P}_k[p_b]' - p_b'\|_{L^\infty([-1,1])} \leq \epsilon \|p_b'\|_{L^\infty([-1,1])}. \quad (124)$$

Clearly, we can also ensure that

$$\|\mathbf{P}_k[g'] - g'\|_{L^\infty([-1,1])} \leq \epsilon \|g'\|_{L^\infty([-1,1])} \quad (125)$$

and

$$\|\mathbf{P}_k[f] - f\|_{L^\infty([-1,1])} \leq \epsilon \|f\|_{L^\infty([-1,1])} \quad (126)$$

with k still chosen independently of G_1 and $|W|$. Now (123) and (125) together with the assumption that $0 < \epsilon < 1$ imply

$$\|\mathbf{P}_k[p_b]\|_{L^\infty([-1,1])} \leq 2 \|p_b\|_{L^\infty([-1,1])} \quad (127)$$

and

$$\|\mathbf{P}_k[g']\|_{L^\infty([-1,1])} \leq 2 \|g'\|_{L^\infty([-1,1])}. \quad (128)$$

It follows readily that

$$\begin{aligned} & \|\mathbf{P}_k[g']\mathbf{P}_k[p_b] - g'p_b\|_{L^\infty([-1,1])} \\ & \leq \|\mathbf{P}_k[p_b]\|_{L^\infty([-1,1])} \|\mathbf{P}_k[g'] - g'\|_{L^\infty([-1,1])} \\ & \quad + \|\mathbf{P}_k[g']\|_{L^\infty([-1,1])} \|\mathbf{P}_k[p_b] - p_b\|_{L^\infty([-1,1])} \\ & \leq 4\epsilon \|g'\|_{L^\infty([-1,1])} \|p_b\|_{L^\infty([-1,1])}. \end{aligned} \quad (129)$$

Now (124) and (129) imply the first inequality in (122), and the second follows from (119) and (120).

Combining (118) with (122) shows that

$$\begin{aligned} & \left| \mathbf{P}_k[p_b]'(x) + \mathbf{P}_k[g'](x) \mathbf{P}_k[p_b](x) - f(x) \right| \\ & \lesssim \epsilon \left(1 + (1 + 4G_1) \min \left\{ 1, \frac{1}{|W|} \right\} \right) \frac{|W|}{G_0} \|f\|_{L^\infty([-1,1])} \end{aligned} \quad (130)$$

for all $x \in [-1, 1]$. If we now let

$$\overline{p_b} = \begin{pmatrix} p_b \left(x_{1,k}^{\text{cheb}} \right) \\ p_b \left(x_{2,k}^{\text{cheb}} \right) \\ \vdots \\ p_b \left(x_{k,k}^{\text{cheb}} \right) \end{pmatrix} \quad \text{and} \quad \overline{f} = \begin{pmatrix} f \left(x_{1,k}^{\text{cheb}} \right) \\ f \left(x_{2,k}^{\text{cheb}} \right) \\ \vdots \\ f \left(x_{k,k}^{\text{cheb}} \right) \end{pmatrix} \quad (131)$$

be the vectors of values of p_b and f at the k -point extremal Chebyshev grid, and define the $k \times k$ matrix \mathcal{G} via

$$\mathcal{G} = \begin{pmatrix} g' \left(x_{1,k}^{\text{cheb}} \right) & & & \\ & g' \left(x_{2,k}^{\text{cheb}} \right) & & \\ & & \ddots & \\ & & & g' \left(x_{k,k}^{\text{cheb}} \right) \end{pmatrix}, \quad (132)$$

then (130) implies that

$$(\mathcal{D}_k + i\mathcal{G}) \overline{p_b} = \overline{f} + \overline{\delta}, \quad (133)$$

where

$$\|\overline{p_b}\| \lesssim \frac{|W|}{G_0} \min \left\{ 1, \frac{1}{|W|} \right\} \|f\|_{L^\infty([-1,1])} \quad (134)$$

and

$$\|\overline{\delta}\| \lesssim \epsilon \left(1 + (1 + 4G_1) \min \left\{ 1, \frac{1}{|W|} \right\} \right) \frac{|W|}{G_0} \|f\|_{L^\infty([-1,1])}. \quad (135)$$

From (134), (135) and the fact that

$$\|\mathcal{D}_k + i\mathcal{G}\| \lesssim \max\{G_1, k^2\}, \quad (136)$$

we see that

$$\|\overline{\delta}\| \lesssim \epsilon \|\mathcal{D}_k + i\mathcal{G}\| \|\overline{p_b}\| \quad (137)$$

regardless of the magnitude of g' . In particular, the left-hand side of (137) is on the order of $(G_1/G_0 + |W|/G_0) \sim G_1/G_0$ when G_1 is large and $G_1/G_0|W|$ when G_1 is small, while the right-hand side is on the order of G_1/G_0 when G_1 is large and $G_1/G_0 k^2 > G_1/G_0|W|$ when G_1 is small. So by Corollary 2, when

we solve the linear system

$$(\mathcal{D}_k + i\mathcal{G}) \bar{x} = \bar{f} \quad (138)$$

via a singular value decomposition which as been truncated at precision on the order of $\epsilon \|\mathcal{D}_k + \mathcal{G}\|$, we obtain a solution \bar{p}_1 such that

$$\|\bar{p}_1\| \lesssim \|\bar{p}_b\| \lesssim \frac{|W|}{G_0} \min \left\{ 1, \frac{1}{|W|} \right\} \|f\|_{L^\infty([-1,1])} \quad (139)$$

and

$$\begin{aligned} \|(\mathcal{D}_k + \mathcal{G}) \bar{p}_1 - \bar{f}\| &\lesssim \epsilon \|\mathcal{D}_k + \mathcal{G}\| \|\bar{p}_b\| \\ &\lesssim \epsilon \frac{|W|}{G_0} \max\{G_1, k^2\} \min \left\{ 1, \frac{1}{|W|} \right\} \|f\|_{L^\infty([-1,1])}. \end{aligned} \quad (140)$$

Now we let p_1 and δ_1 be the k -term Chebyshev expansions whose values at the extremal Chebyshev nodes agree with the values of the vector \bar{p}_1 and those of $(\mathcal{D}_k + \mathcal{G}) \bar{p}_1 - \bar{f}$, respectively. From (139) and (140) and the fact that the Chebyshev polynomials are bounded in $L^\infty([-1, 1])$ norm by 1, we have that

$$\|p_1\|_{L^\infty([-1,1])} \lesssim \frac{|W|}{G_0} \min \left\{ 1, \frac{1}{|W|} \right\} \|f\|_{L^\infty([-1,1])} \quad (141)$$

and

$$\|\delta_1\|_{L^\infty([-1,1])} \lesssim \epsilon \frac{|W|}{G_0} \max\{G_1, k^2\} \min \left\{ 1, \frac{1}{|W|} \right\} \|f\|_{L^\infty([-1,1])}. \quad (142)$$

Moreover, it follows from (138) that

$$p'_1(x_{j,k}^{\text{cheb}}) + ig'(x_{j,k}^{\text{cheb}}) p_1(x_{j,k}^{\text{cheb}}) = f(x_{j,k}^{\text{cheb}}) + \delta_1(x_{j,k}^{\text{cheb}}) \quad (143)$$

for all $j = 1, \dots, k$; that is,

$$\mathbf{P}_k[p'_1 + ig'p_1](x) = \mathbf{P}_k[f + \delta_1](x). \quad (144)$$

But using (125), (126), (141) and the fact that p_1 and δ_1 are k -term Chebyshev expansions, we see that

$$\begin{aligned} &\|\mathbf{P}_k[p'_1 + ig'p_1] - (p'_1 + ig'p_1)\|_{L^\infty([-1,1])} \\ &\leq \epsilon G_1 \|p_1\|_{L^\infty([-1,1])} \\ &\lesssim \epsilon \frac{G_1}{G_0} |W| \min \left\{ 1, \frac{1}{|W|} \right\} \|f\|_{L^\infty([-1,1])} \end{aligned} \quad (145)$$

and

$$\|\mathbf{P}_k[f + \delta_1] - (f + \delta_1)\|_{L^\infty([-1,1])} \leq \epsilon \|f\|_{L^\infty([-1,1])}. \quad (146)$$

It follows from (142), (144), (145) and (146) that

$$|p'_1(x) + ig'(x)p_1(x) - f(x)| \lesssim \epsilon \left(1 + \frac{G_1}{G_0} + \frac{1}{G_0} \max\{G_1, k^2\} \right) |W| \min \left\{ 1, \frac{1}{|W|} \right\} \|f\|_{L^\infty([-1,1])} \quad (147)$$

for all $x \in [-1, 1]$.

To complete our analysis for the case in which $G_0 > 0$, we let

$$I = \int_{-1}^1 f(t) \exp(ig(t)) dt \quad (148)$$

be the true value of the oscillatory integral we hope to compute via the Levin method, and take I_1 to be the estimate

$$I_1 = p_1(1) \exp(ig(1)) - p_1(-1) \exp(ig(-1)). \quad (149)$$

Now

$$\begin{aligned} I_1 - I &= \int_{-1}^1 \frac{d}{dt} (p_1(t) \exp(ig(t))) dt - \int_{-1}^1 f(t) \exp(ig(t)) dt \\ &= \int_{-1}^1 (p'_1(t) + ig'(t)p_1(t) - f(t)) \exp(ig(t)) dt, \end{aligned} \quad (150)$$

and it follows from this and (147) that

$$|I_1 - I| \lesssim \epsilon \left(1 + \frac{G_1}{G_0} + \frac{1}{G_0} \max\{G_1, k^2\} \right) |W| \min \left\{ 1, \frac{1}{|W|} \right\} \|f\|_{L^\infty([-1,1])}. \quad (151)$$

The quantity

$$|W| \min \left\{ 1, \frac{1}{|W|} \right\} \quad (152)$$

is clearly bounded independent of the magnitude of g' . Moreover, G_1/G_0 is small when g' does not vary in magnitude too much over the interval (a reasonable assumption when analyzing an adaptive scheme). So (151) shows that the absolute error in the computed integral is bounded independent of the magnitude of g' , assuming g' does not vary too much over the interval.

We now consider the case in which $G_1 < 1/4$. By invoking Theorem 5, we can find a bandlimited function p_b such that

$$|p'_b(x) + ig'(x)p_b(x) - f(x)| \leq 2\epsilon \left(1 + \frac{G_1}{1 - 2G_1} \right) \|f\|_{L^\infty([-1,1])} \quad (153)$$

for all $x \in [-1, 1]$,

$$\|p_b\|_{L^\infty([-1,1])} \leq \frac{2}{1 - 2G_1} \|f\|_{L^\infty([-1,1])} \quad (154)$$

and

$$\|p'_b\|_{L^\infty([-1,1])} \leq 4 \left(1 + \frac{G_1}{1 - 2G_1}\right) \|f\|_{L^\infty([-1,1])}. \quad (155)$$

Since the bandlimit of p_b is bounded under our assumption on G_1 , the Chebyshev coefficients of p_b are bounded by a rapidly decaying function which is independent of G_1 . Moreover, we can once again choose k independent of G_1 such that (123) through (129) hold. Then, proceeding as we did before shows that

$$\begin{aligned} & \left\| P_k[p_b]' + iP_k[g'] P_k[p_b] - (p'_b + ig'p_b) \right\|_{L^\infty([-1,1])} \\ & \lesssim \epsilon \left(1 + \frac{4G_1}{1 - 2G_1}\right) \|f\|_{L^\infty([-1,1])} \end{aligned} \quad (156)$$

for all $x \in [-1, 1]$. If we define \overline{p}_b , $\overline{\delta}$ and \mathcal{G} as before, then we see that

$$\|\overline{\delta}\| \lesssim \epsilon \left(1 + \frac{4G_1}{1 - 2G_1}\right) \|f\|_{L^\infty([-1,1])} \quad (157)$$

while

$$\|(\mathcal{D}_k + \mathcal{G})\overline{p}_b\| \lesssim \frac{2}{1 - 2G_1} \max\{G_1, k^2\} \|f\|_{L^\infty([-1,1])}, \quad (158)$$

so there is no difficulty in applying Corollary 2 to see that solving (138) via a truncated singular value decomposition yields a solution \overline{p}_1 such that

$$\|\overline{p}_1\| \lesssim \frac{2}{1 - 2G_1} \|f\|_{L^\infty([-1,1])} \quad (159)$$

and

$$\begin{aligned} \|(\mathcal{D}_k + \mathcal{G})\overline{p}_1 - \overline{f}\| & \lesssim \epsilon \|\mathcal{D}_k + \mathcal{G}\| \|\overline{p}_b\| \\ & \lesssim \epsilon \max\{G_1, k^2\} \frac{2}{1 - 2G_1} \|f\|_{L^\infty([-1,1])}. \end{aligned} \quad (160)$$

Defining p_1 and δ_1 as before, we obtain the bound

$$\begin{aligned} & |p'_1(x) + ig'(x)p_1(x) - f(x)| \\ & \lesssim \epsilon \left(\max\{G_1, k^2\} \frac{2}{1 - 2G_1} + \frac{1}{1 - 2G_1} \right) \|f\|_{L^\infty([-1,1])}, \end{aligned} \quad (161)$$

which holds for all $x \in [-1, 1]$. Arguing as before, we see that the absolute error in the computed value of the integral (149) is bounded by a constant multiple of

$$\epsilon \left(\max\{G_1, k^2\} \frac{2}{1 - 2G_1} + \frac{1}{1 - 2G_1} \right) \|f\|_{L^\infty([-1,1])}. \quad (162)$$

Since we are considering an interval on which G_1 is small, the constant in (162) is small as well.

5 The Adaptive Levin Method

In this section, we describe the adaptive Levin method for the numerical calculation of the integral

$$\int_a^b \exp(ig(x))f(x) dx. \quad (163)$$

Trivial modifications allow for the evaluation of

$$\int_a^b \cos(g(x))f(x) dx \quad \text{or} \quad \int_a^b \sin(g(x))f(x) dx \quad (164)$$

instead.

Before detailing the algorithm proper, we describe a subroutine which estimates the value of

$$\int_{a_0}^{b_0} \exp(ig(x))f(x) dx, \quad (165)$$

where $[a_0, b_0]$ is a subinterval of $[a, b]$. It takes as input the interval $[a_0, b_0]$, an integer k which controls the number of Chebyshev nodes used to discretize the Levin equation and an external subroutine for evaluating the functions f and g . The subroutine proceeds as follows:

1. Use the external subroutine supplied by the user to evaluate the functions f and g at the extremal Chebyshev nodes $x_{1,k}^{\text{cheb}}, x_{2,k}^{\text{cheb}}, \dots, x_{k,k}^{\text{cheb}}$.
2. Calculate approximate values

$$\widetilde{g' \left(x_{1,k}^{\text{cheb}} \right)}, \dots, \widetilde{g' \left(x_{k,k}^{\text{cheb}} \right)}, \quad (166)$$

of the derivatives of the function g at the extremal Chebyshev nodes by applying the spectral differential matrix \mathcal{D}_k to the vector of values of g ; that is, via the formula

$$\begin{pmatrix} \widetilde{g' \left(x_{1,k}^{\text{cheb}} \right)} \\ \widetilde{g' \left(x_{2,k}^{\text{cheb}} \right)} \\ \vdots \\ \widetilde{g' \left(x_{k,k}^{\text{cheb}} \right)} \end{pmatrix} = \mathcal{D}_k \begin{pmatrix} g \left(x_{1,k}^{\text{cheb}} \right) \\ g \left(x_{2,k}^{\text{cheb}} \right) \\ \vdots \\ g \left(x_{k,k}^{\text{cheb}} \right) \end{pmatrix}. \quad (167)$$

3. Form the matrix

$$\mathcal{A} = \mathcal{D}_k + i \begin{pmatrix} \widetilde{g'(x_{1,k}^{\text{cheb}})} & & & \\ & \widetilde{g'(x_{2,k}^{\text{cheb}})} & & \\ & & \ddots & \\ & & & \widetilde{g'(x_{k,k}^{\text{cheb}})} \end{pmatrix}. \quad (168)$$

4. Construct a singular value decomposition

$$\mathcal{A} = (\overline{u_1} \ \overline{u_2} \ \cdots \ \overline{u_k}) \begin{pmatrix} \sigma_1 & & & \\ & \sigma_2 & & \\ & & \ddots & \\ & & & \sigma_k \end{pmatrix} (\overline{v_1} \ \overline{v_2} \ \cdots \ \overline{v_k})^* \quad (169)$$

of the matrix \mathcal{A} .

5. Find the least integer $1 \leq l \leq k$ such that $\sigma_l \geq \|\mathcal{A}\|_{\epsilon_0}$, where ϵ_0 is machine zero. If no such integer exists, return the estimate 0 for (165).
6. Let

$$\begin{pmatrix} \widetilde{p(x_{1,k}^{\text{cheb}})} \\ \widetilde{p(x_{2,k}^{\text{cheb}})} \\ \vdots \\ \widetilde{p(x_{k,k}^{\text{cheb}})} \end{pmatrix} = (\overline{v_1} \ \cdots \ \overline{v_l}) \begin{pmatrix} \frac{1}{\sigma_1} & & & \\ & \frac{1}{\sigma_2} & & \\ & & \ddots & \\ & & & \frac{1}{\sigma_l} \end{pmatrix} (\overline{u_1} \ \cdots \ \overline{u_l})^* \begin{pmatrix} f(x_1) \\ f(x_2) \\ \vdots \\ f(x_k) \end{pmatrix}.$$

The entries of this vector approximate the values of a function p such that

$$\frac{d}{dx} (p(x) \exp(ig(x))) = f(x) \exp(ig(x)) \quad (170)$$

at the external Chebyshev nodes on $[a_0, b_0]$.

7. Return the estimate

$$\widetilde{p(x_{k,k}^{\text{cheb}})} \exp(ig(x_k)) - \widetilde{p(x_{1,k}^{\text{cheb}})} \exp(ig(x_1)) \quad (171)$$

for the value of (165).

The algorithm proper takes as input a tolerance parameter $\epsilon > 0$, the endpoints $a < b$ of the integration domain, an integer k specifying the number of Chebyshev nodes used to discretize the Levin equation on each subinterval considered, and an external subroutine which returns the values of the functions f and g at a specified collection of points. It maintains an estimated value val for (163) and a list of intervals. Initially, the list of intervals contains only

$[a, b]$ and the value of the estimate is set to 0. As long as the list of intervals is nonempty the following steps are repeated:

1. Remove an entry $[a_0, b_0]$ from the list of intervals.
2. Calculate an estimate val_0 of

$$\int_{a_0}^{b_0} \exp(ig(x))f(x) dx \quad (172)$$

using the subprocedure described above.

3. Calculate estimates val_L and val_R of

$$\int_{a_0}^{c_0} \exp(ig(x))f(x) dx \quad \text{and} \quad \int_{c_0}^{b_0} \exp(ig(x))f(x) dx, \quad (173)$$

where $c_0 = (a_0 + b_0)/2$, using the subprocedure described above.

4. If $|val_0 - val_L - val_R| < \epsilon$, then update the estimate val by letting $val = val + val_0$. Otherwise, add the intervals $[a_0, c_0]$ and $[c_0, b_0]$ to the list of intervals.

In the end, the procedure returns the estimate val for (163). Because the condition number of the oscillatory integral (163) increases with the magnitude of g , some loss of accuracy is expected when calculating its value numerically. In the case of the adaptive Levin method, the principal loss of accuracy occurs when exponentials of large magnitude are evaluated in (171). Of course, the magnitudes of many integrals of the form (163) decrease with the magnitude g , with the consequence that the absolute error in the calculated value of (163) often remains constant or even decays as the magnitude of g increases.

Remark 2. *The truncated singular value decomposition is quite expensive. In our implementation of the adaptive Levin method, we used a rank-revealing QR decomposition in lieu of the truncated singular value decomposition to solve the linear system which results from discretizing the ordinary differential equation. This was found to be about 5 times faster and leads to no apparent loss in accuracy.*

6 Numerical experiments

In this section, we present the results of numerical experiments which were conducted to illustrate the properties of the algorithm of this article. The code for these experiments was written in Fortran and compiled with version 12.10 of the GNU Fortran compiler. They were performed on a desktop computer equipped with an AMD Ryzen 3900X processor and 32MB of memory. No attempt was made to parallelize our code. We used a 12-point Chebyshev spectral method in our implementation of the adaptive Levin scheme (i.e., the parameter k was taken to be 12). As discussed in Section 5, the condition

number of evaluation of most integrals of the form

$$\int_a^b \exp(ig(x))f(x) dx \quad (174)$$

increases with the magnitude of g' . This is often offset by a commensurate decrease in the magnitude of the integral with the consequence that, in most cases, it is reasonable to expect absolute errors in the calculated values of (174) to be largely independent of the magnitude of g' .

In some of these experiments, we compared the results of the algorithm of this paper with those of an adaptive Gaussian quadrature code for evaluating integrals of the form

$$\int_a^b f(x) dx, \quad -\infty < a < b < \infty. \quad (175)$$

Our implementation of this algorithm is written in Fortran and is quite standard. It maintains a list of intervals, which is initialized with the single interval $[a, b]$, and a running tally of the value of the integral, which is initialized to zero. As long as the list of intervals is nonempty, the algorithm removes one interval $[a_0, b_0]$ from the list, compares the value of

$$\int_{a_0}^{b_0} f(x) dx \quad (176)$$

as computed by a 30-point Gauss-Legendre quadrature rule to the value of the sum

$$\int_{a_0}^{(a_0+b_0)/2} f(x) dx + \int_{(a_0+b_0)/2}^{b_0} f(x) dx, \quad (177)$$

where each integral is separately estimated with a 30-point Gauss-Legendre rule. If the difference is larger than ϵ , where ϵ is a tolerance parameter supplied by the user, then the intervals $[a_0, (a_0 + b_0)/2]$ and $[(a_0 + b_0)/2, b_0]$ are placed in the list of intervals. Otherwise, the value of (176) is added to the running tally of the value of the integral (175). In all of the experiments described here, the tolerance parameter for the adaptive Gaussian quadrature code was taken to be $\epsilon = 10^{-15}$. We found it necessary to set the tolerance parameter for adaptive Gaussian quadrature to be somewhat smaller than that for the adaptive Levin method in order to obtain accurate results from the former. We used a 30-point Gauss-Legendre rule because we found it to be more efficient than rules of other orders in most cases.

The experiments of Subsection 6.4 concern Bessel functions, those of Subsection 6.5 involve the associated Legendre functions and the experiments of Subsection 6.6 concern Hermite polynomials. In order to apply the adaptive Levin method to integrals involving these functions, we constructed phase function representations of them via the method of [15]. That algorithm applies to

second order linear ordinary differential equations of the form

$$y''(x) + q(x)y(x) = 0, \quad a < x < b, \quad (178)$$

where the coefficient q is real-valued and slowly-varying. We note that essentially any second order differential equation, including the differential equation defining the associated Legendre functions and Bessel's differential equation, can be put into the form (178) via a simple transformation. The method of [15] constructs a piecewise Chebyshev expansion representing a slowly-varying phase function ψ such that

$$\frac{\exp(i\psi(x))}{\sqrt{\psi'(x)}} \quad \text{and} \quad \frac{\exp(-i\psi(x))}{\sqrt{\psi'(x)}} \quad (179)$$

constitute a basis in the space of solutions of (178). The derivative of the phase function is uniquely determined, but the phase function itself is only defined up to a constant. We typically use this degree of freedom to ensure that either

$$\frac{\sin(\psi(x))}{\sqrt{\psi'(x)}} \quad \text{or} \quad \frac{\cos(\psi(x))}{\sqrt{\psi'(x)}} \quad (180)$$

represent the special function we wish to integrate.

6.1 Certain integrals involving elementary functions for which explicit formulas are available

In the experiments described in this subsection, we considered the integrals

$$\begin{aligned} I_1(\lambda) &= \int_{-1}^1 \cos(\lambda \arctan(x)) \frac{1}{1+x^2} dx = \frac{2}{\lambda} \sin\left(\frac{\pi\lambda}{4}\right), \\ I_2(\lambda) &= \int_0^\infty \frac{\exp(i\lambda x^2)}{\sqrt{x}} dx = \exp\left(\frac{\pi i}{8}\right) \frac{2\Gamma\left(\frac{5}{4}\right)}{\lambda^{\frac{1}{4}}}, \\ I_3(\lambda) &= \int_0^1 \exp\left(\frac{i\lambda}{\sqrt{x}}\right) \frac{1}{x} dx = 2\Gamma(0, -i\lambda) \quad \text{and} \\ I_4(\lambda) &= \int_0^{10} \exp(i\lambda \exp(x)) \exp(x) dx = \frac{i}{\lambda} (\exp(i\lambda) - \exp(i \exp(10) \lambda)). \end{aligned}$$

All of the above formulas can be found in [22].

We proceeded by first sampling $l = 200$ equispaced points x_1, \dots, x_l in the interval $[1, 7]$. Then, we used the adaptive Levin method to evaluate the integrals appearing above for each $\lambda = 10^{x_1}, 10^{x_2}, \dots, 10^{x_l}$. Figures 1 and 2 give the time require to evaluate these integrals and the absolute errors in the obtained values.

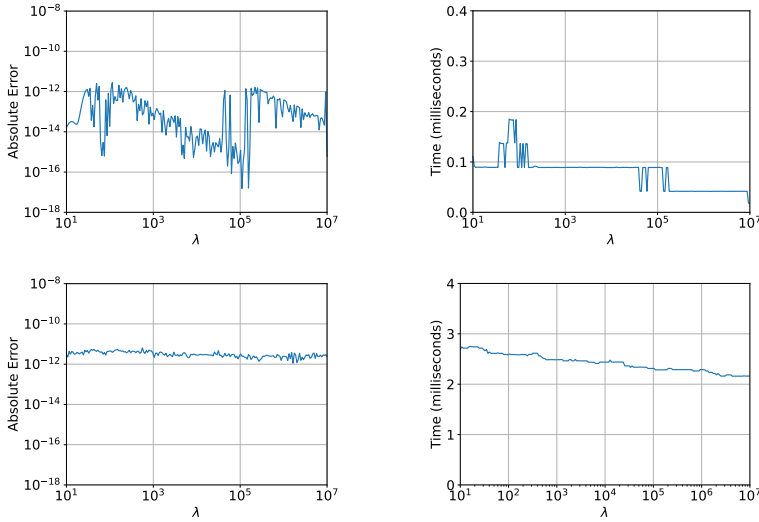


Fig. 1: The results of the first two experiments of Section 6.1. The first row of plots pertains to the integral I_1 and the second to I_2 . Each plot on the left gives the error in the value of the integral computed via the adaptive Levin method as a function of λ , while each plot on the right gives the running time in milliseconds as a function of λ .

6.2 Certain other integrals involving elementary functions

In the experiments of this subsection, we evaluated the integrals

$$\begin{aligned}
 I_5(\lambda) &= \int_0^1 \exp(i\lambda x^2) \exp(-x) x \, dx, \\
 I_6(\lambda) &= \int_{-1}^1 \exp(i\lambda x^2) (1 + x^2) \, dx, \\
 I_7(\lambda) &= \int_{-4}^4 \exp(i\lambda x^2) \, dx \quad \text{and} \\
 I_8(\lambda) &= \int_{-1}^1 \exp(i\lambda x^4) \frac{1}{0.01 + x^4} \, dx.
 \end{aligned} \tag{181}$$

We considered various ranges of values of λ . We randomly sampled 200 values of λ in each range and, then, for each such value of λ , we calculated I_5 , I_6 , I_7 and I_8 using both the adaptive Levin algorithm and our adaptive Gaussian quadrature code. The time taken by each method was measured, and the absolute differences between the values of the integrals calculated with each method recorded. Table 1 gives the result. Each row gives the results for one integral and range of values of λ .

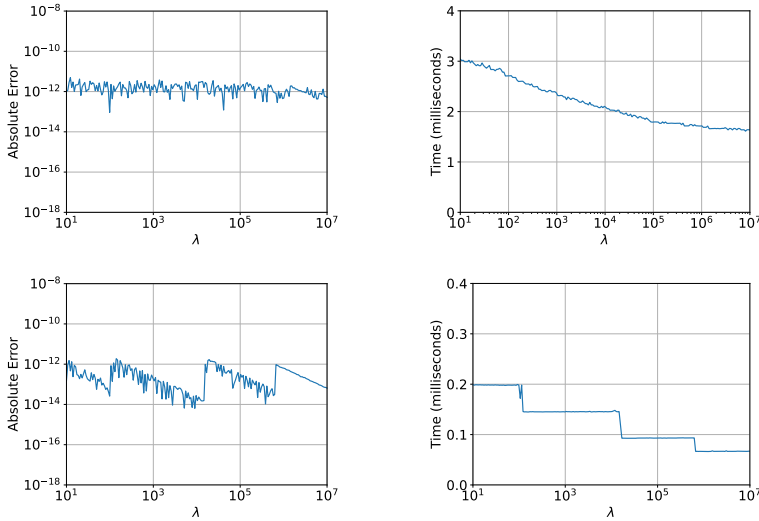


Fig. 2: The results of the last two experiments of Section 6.1. The first row of plots pertains to the integral I_3 and the second to I_4 . Each plot on the left gives the error in the value of the integral computed via the adaptive Levin method as a function of λ , while each plot on the right gives the running time in milliseconds as a function of λ .

6.3 Behavior in the presence of a stationary point

In the experiments of this subsection, we considered the integral

$$I_9(\lambda, m) = \int_{-1}^1 \exp(i\lambda x^m) \frac{\cos(x)}{1+x^2} dx \quad (182)$$

in order to understand the behavior of the adaptive Levin method in the presence of a stationary point.

In the first experiment, we sampled $l = 200$ equispaced points x_1, \dots, x_l in the interval $[1, 7]$ and, for each $\lambda = 10^{x_1}, 10^{x_2}, \dots, 10^{x_l}$ and $m = 2, 3, \dots, 9$, we evaluated $I_9(\lambda, m)$ twice using the adaptive Levin method. The first time the scheme was executed, the tolerance parameter taken to be $\epsilon = 10^{-12}$. The second time, we set $\epsilon = 10^{-7}$. The results are shown in the first two rows of Figure 3. The first column gives the results for $\epsilon = 10^{-7}$ and the second for $\epsilon = 10^{-12}$. The plots in the first row show the number of subintervals in the adaptively determined subdivision of $[-1, 1]$ used to compute the integral as a function of λ for $m = 2, 3, 4, 5$, while those in the second give the absolute error in the computed value of the integral as a function of λ for $m = 2, 3, 4, 5$.

In a second experiment, for each $m = 2, 3, 4, \dots, 40$ and $\lambda = 10^2, 10^3, 10^4, 10^5$ we evaluated $I_9(\lambda, m)$ twice using the adaptive Levin method. In the first run, the tolerance parameter was taken to be $\epsilon = 10^{-12}$ and, in the second, it was

Integral	Range of λ	Avg Time Adap Levin	Avg Time Adap Gauss	Ratio	Max Observed Difference
I_5	$10^0 - 10^1$	4.83×10^{-05}	2.23×10^{-06}	0.05	9.94×10^{-13}
	$10^1 - 10^2$	9.16×10^{-05}	5.93×10^{-06}	0.06	1.32×10^{-12}
	$10^2 - 10^3$	1.23×10^{-04}	4.71×10^{-05}	0.38	1.01×10^{-12}
	$10^3 - 10^4$	1.58×10^{-04}	4.15×10^{-04}	2.64	7.53×10^{-13}
	$10^4 - 10^5$	2.02×10^{-04}	4.26×10^{-03}	21.12	9.99×10^{-13}
	$10^5 - 10^6$	2.29×10^{-04}	3.99×10^{-02}	173.87	1.00×10^{-12}
	$10^6 - 10^7$	2.51×10^{-04}	3.71×10^{-01}	1476.94	4.00×10^{-13}
I_6	$10^0 - 10^1$	1.38×10^{-04}	2.29×10^{-06}	0.02	1.94×10^{-12}
	$10^1 - 10^2$	2.88×10^{-04}	1.38×10^{-05}	0.05	1.97×10^{-12}
	$10^2 - 10^3$	4.17×10^{-04}	1.07×10^{-04}	0.26	3.58×10^{-12}
	$10^3 - 10^4$	4.74×10^{-04}	9.00×10^{-04}	1.90	3.32×10^{-12}
	$10^4 - 10^5$	5.25×10^{-04}	8.84×10^{-03}	16.85	2.20×10^{-12}
	$10^5 - 10^6$	5.77×10^{-04}	8.05×10^{-02}	139.52	3.53×10^{-12}
	$10^6 - 10^7$	6.44×10^{-04}	8.01×10^{-01}	1243.52	2.57×10^{-12}
I_7	$10^0 - 10^1$	3.61×10^{-04}	3.03×10^{-05}	0.08	2.57×10^{-12}
	$10^1 - 10^2$	4.84×10^{-04}	2.44×10^{-04}	0.51	2.97×10^{-12}
	$10^2 - 10^3$	5.32×10^{-04}	2.31×10^{-03}	4.34	3.67×10^{-12}
	$10^3 - 10^4$	5.86×10^{-04}	2.24×10^{-02}	38.15	3.41×10^{-12}
	$10^4 - 10^5$	6.35×10^{-04}	2.21×10^{-01}	347.36	2.52×10^{-12}
	$10^5 - 10^6$	6.93×10^{-04}	2.31×10^{-00}	3337.39	3.29×10^{-12}
	$10^6 - 10^7$	7.61×10^{-04}	2.66×10^{-01}	34967.12	5.68×10^{-12}
I_8	$10^0 - 10^1$	8.66×10^{-04}	4.26×10^{-05}	0.05	3.48×10^{-12}
	$10^1 - 10^2$	7.32×10^{-04}	1.70×10^{-04}	0.23	6.57×10^{-12}
	$10^2 - 10^3$	7.58×10^{-04}	1.43×10^{-03}	1.88	4.17×10^{-12}
	$10^3 - 10^4$	7.49×10^{-04}	1.36×10^{-02}	18.09	7.30×10^{-12}
	$10^4 - 10^5$	7.41×10^{-04}	1.31×10^{-01}	177.18	6.40×10^{-12}
	$10^5 - 10^6$	7.57×10^{-04}	1.19×10^{-00}	1570.01	3.62×10^{-12}
	$10^6 - 10^7$	8.23×10^{-04}	1.37×10^{-01}	16697.05	3.76×10^{-12}

Table 1: The results of the experiments of Section 6.2 in which the performance of the adaptive Levin method was compared with the performance of an adaptive Gaussian quadrature scheme. Each row corresponds to one of the integrals $I_5(\lambda)$, $I_6(\lambda)$, $I_7(\lambda)$ or $I_8(\lambda)$ and to one range of values of λ . The average time taken by the adaptive Levin method and by an adaptive Gaussian quadrature scheme, the ratio of the average time taken by the adaptive Gaussian quadrature algorithm to the average time taken by the adaptive Levin method, and the maximum observed difference in the values of the integrals computed using each method are reported.

$\epsilon = 10^{-7}$. The results appear in the third row of Figure 3. Each plot there gives the number of subintervals in the adaptive subdivision of $[-1, 1]$ formed by our algorithm as a function of m for each of the values of λ considered. The plot on the left corresponds to $\epsilon = 10^{-12}$ and the plot on the right to $\epsilon = 10^{-7}$.

We see that, when $\epsilon = 10^{-12}$, the number of subintervals in the adaptive subdivision of $[-1, 1]$ formed by the adaptive Levin method varies only slightly with λ and is largely independent of m . However, when $\epsilon = 10^{-7}$, the number of subintervals grows roughly logarithmically with λ and decreases with m for

small values of m . It is essentially independent of m for moderate to large values of m .

This behavior can be understood in light of the the analysis presented in Section 3. Theorem 5 implies that the Levin method will yield an accurate result on subintervals of the form $[-\delta, \delta]$ provided g' is sufficiently small there. Theorem 4 indicates that the Levin method will yield an accurate result on any subinterval of $[-1, 1]$ which is bounded away from 0 provided the ratio of

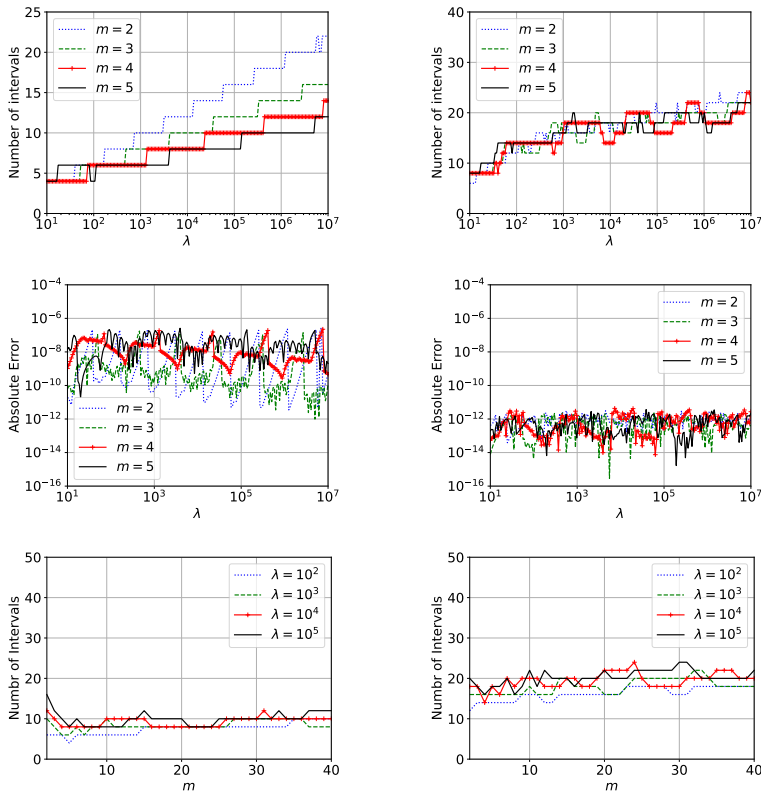


Fig. 3: The results of the experiments of Section 6.3. The plots in the first row give the number of subintervals in the adaptive discretization of $[-1, 1]$ formed in the course of evaluating $I_9(\lambda, m)$ as a function of λ for $m = 2, 3, 4, 5$; those in the second row give the absolute error in the calculated error in the value of $I_9(\lambda, m)$ as a function of λ for $m = 2, 3, 4, 5$; and the plots in the third row show the number of subintervals in the adaptive discretization of $[-1, 1]$ as a function of m for $\lambda = 10^2, 10^3, 10^4, 10^5$. The plots in the column on the left concern experiments executed with the precision parameter ϵ taken to be 10^{-7} , while those on the right correspond to $\epsilon = 10^{-12}$.

the maximum to minimum value of g' is small and

$$h(z) = f(u^{-1}(z)) \frac{du^{-1}}{dz}(z) = \frac{f(\operatorname{sign}(z)|z|^{\frac{1}{m}})}{m|z|^{1-\frac{1}{m}}} \quad (183)$$

can be represented via a well-behaved function with a small bandlimit there. That h can be represented by a function with small bandlimit is more-or-less equivalent to the requirement that h be represented via a Chebyshev expansion of small fixed order. We expect the adaptive Levin method to subdivide $[-1, 1]$ until one or both of Theorems 4 and 5 apply to each of the resulting subintervals.

Since $g'(x) = \lambda m x^{m-1}$, in order for $|g'(x)|$ to be bounded by a constant C on $[-\delta, \delta]$, we must have

$$\delta < \left(\frac{C}{m\lambda} \right)^{\frac{1}{m-1}}. \quad (184)$$

So we expect the adaptive Levin method to divide $[-1, 1]$ into at least

$$\log(\delta) \sim \frac{\log(m\lambda)}{m-1} \quad (185)$$

subintervals. The algorithm will further divide the subintervals contained in $[-1, -\delta]$ and $[\delta, 1]$ until, on each of the resulting subintervals, the ratio of the maximum to minimum value of g' is small and h is well-represented via a Chebyshev expansion of small fixed order. The number of subintervals required for these conditions to be met depends only weakly on m and λ . The dependence on λ arises because the greater the distance δ between these intervals and 0, the fewer subdivisions required, and the distance δ depends on λ .

When $\epsilon = 10^{-12}$, the the cost of our algorithm is dominated by the need to represent $h(z)$. This depends only weakly on m and λ , and this behavior is reflected in the results shown in Figure 3. They indicate that the cost of the adaptive Levin method grows only very slowly with λ in this case, and that it is essentially independent of m .

When $\epsilon = 10^{-7}$, the difficulty of representing $h(x)$ is lower, and the running time our algorithm is dominated by the number of subdivisions needed to ensure δ is sufficiently small, at least when m is small. This is on the order of $\log(m\lambda)/(m-1)$, and we see this behavior in the plot appearing on the left-hand side of the first row of Figure 3. As m increases, though, the cost of representing $h(z)$ begins to dominate the running time of the algorithm and it ceases to depends strongly on λ . This is reflected in plot appearing on the lower-left corner of Figure 3.

The behavior of the adaptive Levin method in the presence of stationary points is somewhat complicated, but from this analysis and the experiments described above, it is safe to conclude that at worst the algorithm grows logarithmically with the frequency of g' .

6.4 Certain integrals involving the Bessel functions

In the experiments described in this subsection, we used the adaptive Levin method to evaluate the integrals

$$\begin{aligned}
 I_{10}(\nu) &= \int_0^\infty \frac{J_\nu(x)}{\sqrt{x}} dx = \frac{\Gamma\left(\frac{\nu}{2} + \frac{1}{4}\right)}{\sqrt{2} \Gamma\left(\frac{\nu}{2} + \frac{3}{4}\right)}, \\
 I_{11}(\lambda) &= \int_0^\infty Y_{\frac{1}{2}}(\lambda x) \exp(-x) dx = -\frac{\sqrt{\sqrt{\lambda^2 + 1} + 1}}{\sqrt{\lambda^3 + \lambda}}, \\
 I_{12}(\lambda) &= \int_0^{\frac{\pi}{2}} J_{2\lambda}(2\lambda \cos(x)) dx = \frac{\pi}{2} J_\lambda^2(\lambda) \quad \text{and} \\
 I_{13}(\lambda) &= \int_0^\infty J_0(\lambda x) J_{\frac{1}{2}}(\lambda x) \exp(-x) \sqrt{x} dx = \sqrt{\frac{-1 + \sqrt{1 + 4\lambda^2}}{\pi\lambda + 4\pi\lambda^3}}.
 \end{aligned} \tag{186}$$

Each of the above formulas can be found either in [22] or [23].

In the first experiment, we sampled $l = 200$ equispaced points x_1, x_2, \dots, x_l in the interval $[1, 7]$. Then, for each $\nu = 10^{x_1}, \dots, 10^{x_l}$, we constructed a phase function for the normal form

$$y''(x) + \left(1 + \frac{\frac{1}{4} - \nu^2}{x^2}\right) y(x) = 0 \tag{187}$$

of Bessel's differential equation using the algorithm of [15]. This gave us the following representations of the Bessel function of the first and second kinds of order λ :

$$J_\nu(x) = \sqrt{\frac{2}{\pi x}} \frac{\sin(\psi_\nu^{\text{bes}}(x))}{\sqrt{\frac{d}{dx} \psi_\nu^{\text{bes}}(x)}} \quad \text{and} \quad Y_\nu(x) = \sqrt{\frac{2}{\pi x}} \frac{\cos(\psi_\nu^{\text{bes}}(x))}{\sqrt{\frac{d}{dx} \psi_\nu^{\text{bes}}(x)}}. \tag{188}$$

The first of these representations was used, together with the adaptive Levin method, to evaluate $I_{10}(\nu)$. More explicitly, we took the input functions for the adaptive Levin method to be

$$g(x) = \psi_\nu^{\text{bes}}(x) \quad \text{and} \quad f(x) = \frac{1}{x} \sqrt{\frac{2}{\pi \frac{d}{dx} \psi_\nu^{\text{bes}}(x)}}. \tag{189}$$

The results are given in the first row of Figure 4. Note that for this experiment, we report the time taken by the adaptive Levin method and the time required to construct the phase function separately.

We began our second experiment by sampling $l = 200$ equispaced points x_1, \dots, x_l in the interval $[1, 7]$. Then, for each $\lambda = 10^{x_1}, 10^{x_2}, \dots, 10^{x_l}$, we constructed the phase function $\psi_{1/2}^{\text{bes}}$ and executed the adaptive Levin method with the input functions taken to be

$$g(x) = \psi_{1/2}^{\text{bes}}(\lambda x) \quad \text{and} \quad f(x) = \sqrt{\frac{2}{\pi}} \exp(-x) \sqrt{\frac{1}{\lambda x \frac{d}{dx} \psi_{1/2}^{\text{bes}}(\lambda x)}} \tag{190}$$

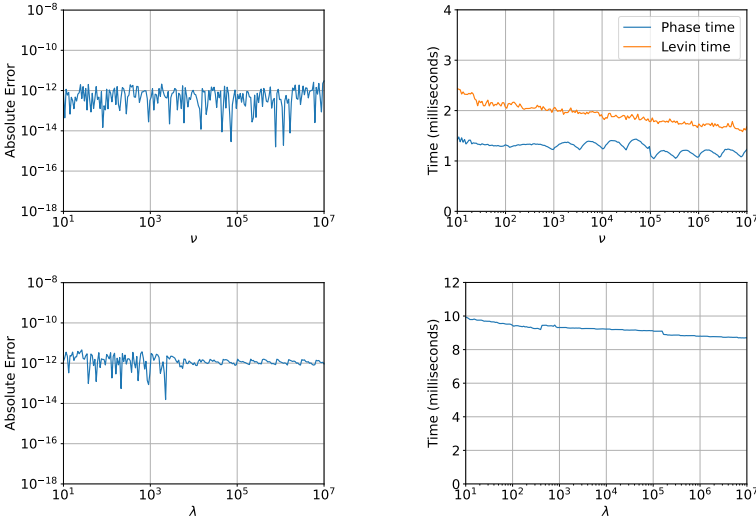


Fig. 4: The results of the first two experiments of Section 6.4. In the first row, the plot on the left gives the absolute error in the calculation of the integral $I_{10}(\nu)$ as a function ν and the plot on the right shows the time take by the adaptive Levin method and the time taken to construct the phase function as functions of ν . The plot at bottom left gives the absolute error in the obtained value of $I_{11}(\lambda)$ as a function of λ , and the bottom-right plot gives the time required to compute $I_{11}(\lambda)$, including the time required to construct any necessary phase functions, as a function of λ .

in order to evaluate $I_{11}(\lambda)$. The results are shown in the second row of Figure 4. The reported times include the cost of constructing the phase function as well as the time required by the adaptive Levin method.

We began our third experiment regarding Bessel functions by sampling $l = 200$ equispaced points x_1, \dots, x_l in the interval $[1, 7]$. Then, for each $\lambda = 10^{x_1}, 10^{x_2}, \dots, 10^{x_l}$, we constructed a phase function $\psi_{2\lambda}^{\text{bes}}$ representing the Bessel functions of order 2λ and used the adaptive Levin method to evaluate $I_{12}(\lambda)$; the input functions were taken to be

$$g(x) = \psi_{2\lambda}^{\text{bes}}(2\lambda \cos(x)) \quad \text{and} \quad f(x) = \sqrt{\frac{2}{\pi}} \sqrt{\frac{1}{2\lambda \cos(x) \frac{d}{dx} \psi_{2\lambda}^{\text{bes}}(2\lambda \cos(x))}}.$$

The results are shown in the first row of Figure 5. Once again, the reported times include the cost of constructing the necessary phase functions as well as the time required by the adaptive Levin method.

In our fourth experiment concerning Bessel functions, we first sampled $l = 200$ equispaced points x_1, \dots, x_l in the interval $[1, 7]$. Then, for each $\lambda = 10^{x_1}, 10^{x_2}, \dots, 10^{x_l}$, we constructed the phase functions ψ_0^{bes} and $\psi_{1/2}^{\text{bes}}$, one representing the Bessel functions of order 0 and the other the Bessel functions

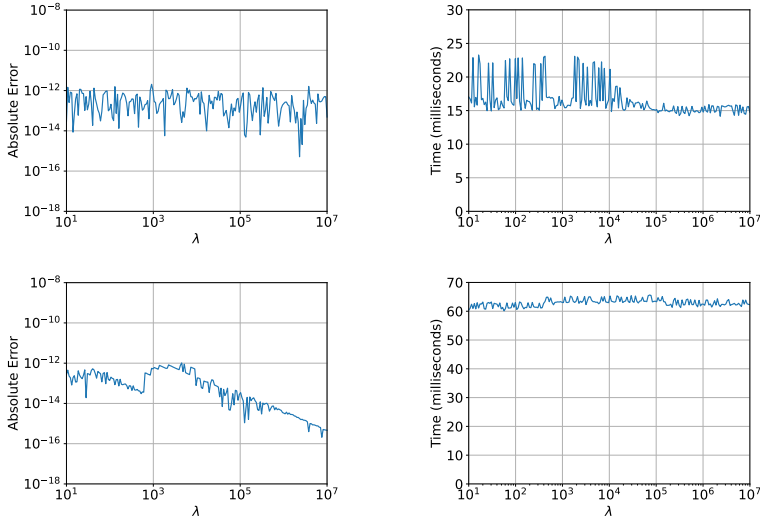


Fig. 5: The results of the last two experiments of Section 6.4. The first row pertains to $I_{12}(\lambda)$ while the second concerns $I_{13}(\lambda)$. In each row, the plot on the left gives the absolute error in the calculation of the integral as a function of λ and the plot on the right shows the total time required to compute the integral via the adaptive Levin method and to construct any necessary phase functions as a function of λ .

of order $1/2$. Since

$$I_{13}(\lambda) = \frac{2}{\pi} \int_0^\infty \frac{\sin(\psi_0^{\text{bes}}(\lambda x))}{\sqrt{\lambda x \frac{d}{dx} \psi_0^{\text{bes}}(\lambda x)}} \frac{\sin(\psi_{1/2}^{\text{bes}}(\lambda x))}{\sqrt{\lambda x \frac{d}{dx} \psi_{1/2}^{\text{bes}}(\lambda x)}} \exp(-x) \sqrt{x} dx \quad (191)$$

and

$$\sin(x) \sin(y) = \frac{\cos(x - y) - \cos(x + y)}{2}, \quad (192)$$

we were able to compute I_{13} via the formula

$$I_{13}(\lambda) = \frac{2}{\lambda \pi} \frac{I_{13a}(\lambda) - I_{13b}(\lambda)}{2}, \quad (193)$$

where

$$I_{13a}(\lambda) = \int_0^\infty \frac{\cos(\psi_{1/2}^{\text{bes}}(x) - \psi_0^{\text{bes}}(x))}{\sqrt{x \frac{d}{dx} \psi_0^{\text{bes}}(x) \frac{d}{dx} \psi_{1/2}^{\text{bes}}(x)}} \exp(-x) dx \quad (194)$$

and

$$I_{13b}(\lambda) = \int_0^\infty \frac{\cos(\psi_0^{\text{bes}}(x) + \psi_{1/2}^{\text{bes}}(x))}{\sqrt{x \frac{d}{dx} \psi_0^{\text{bes}}(x) \frac{d}{dx} \psi_{1/2}^{\text{bes}}(x)}} \exp(-x) dx. \quad (195)$$

The integrals I_{13a} and I_{13b} were, of course, evaluated using the adaptive Levin method. The results are shown in the second row of Figure 5. The reported times include the cost of constructing the two necessary phase functions as well as the time required by the adaptive Levin method.

6.5 Certain integrals involving the associated Legendre functions

In the experiments described in this subsection, we used the adaptive Levin method to evaluate the integrals

$$\begin{aligned} I_{15}(\nu, \mu) &= \int_0^1 \tilde{P}_\nu^\mu(x) (1-x^2)^{\frac{\mu}{2}} dx \\ &= \sqrt{\left(\nu + \frac{1}{2}\right) \frac{\Gamma(\nu + \mu + 1)}{\Gamma(\nu - \mu + 1)}} \frac{(-1)\mu 2^{-\mu-1} \sqrt{\pi}}{\Gamma\left(1 + \frac{\mu}{2} - \frac{\nu}{2}\right) \Gamma\left(\frac{3}{2} + \frac{\mu}{2} + \frac{\nu}{2}\right)}, \\ I_{16}(\lambda) &= \int_0^1 \tilde{P}_\lambda^{\frac{1}{2}}(x) \tilde{Q}_\lambda^{\frac{1}{2}}(x) dx \quad \text{and} \\ I_{17}(\lambda) &= \int_0^{\frac{\pi}{2}} \tilde{P}_\lambda^1(\cos(x)) dx. \end{aligned}$$

Here, we use \tilde{P}_ν^μ and \tilde{Q}_ν^μ to denote normalized version of the Ferrer's functions of the first and second kinds of degree ν and order μ . For $\nu \geq \mu$, the usual Ferrer's function P_ν^μ is the the unique solution of the associated Legendre differential equation

$$(1-x^2)y''(x) - 2xy'(x) + \left(\nu(\nu+1) - \frac{\mu^2}{1-x^2}\right)y(x) = 0 \quad (196)$$

which is regular at the singular point $x = 1$ and such that $P_\nu^\mu(1) = 1$. Because, for most values of the parameters ν and μ , P_ν^μ is exponentially decaying on some part of the interval $[0, 1]$, it can take on extremely large values. Accordingly, we prefer to work with the normalized Ferrer's function

$$\tilde{P}_\nu^\mu(x) = \sqrt{\left(\nu + \frac{1}{2}\right) \frac{\Gamma(\nu + \mu + 1)}{\Gamma(\nu - \mu + 1)}} P_\nu^\mu(x) \quad (197)$$

whose $L^2(-1, 1)$ is 1 when $n \geq m$ are integers. The Ferrer's function Q_ν^μ of the second kind is (essentially) $\pi/2$ times the Hilbert transform of P_ν^μ and we define its normalized version via

$$\tilde{Q}_\nu^\mu(x) = \frac{2}{\pi} \sqrt{\left(\nu + \frac{1}{2}\right) \frac{\Gamma(\nu + \mu + 1)}{\Gamma(\nu - \mu + 1)}} Q_\nu^\mu(x). \quad (198)$$

We refer the reader to Section 5.15 of [24] for a thorough discussion of of the Ferrer's functions.

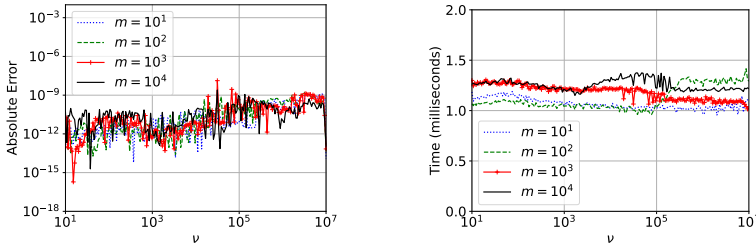


Fig. 6: The results of the first experiment of Section 6.5. The plots give the error in the calculated value of $I_{15}(m + \nu, m)$ and the time required to calculate it via the adaptive Levin method (including the time spent constructing the phase function) as functions of ν for $m = 10, 10^2, 10^3, 10^4$.

Because (196) has singular points at ± 1 , it is convenient to introduce the change of variables

$$z(w) = y(\tanh(w)), \quad (199)$$

which yields the new differential equation

$$z''(w) + (\nu(\nu + 1) \operatorname{sech}^2(w) - \mu^2) z(w) = 0. \quad (200)$$

Applying the algorithm of [15] to (200) gives us the representations

$$\begin{aligned} \frac{\sin(\psi_{\nu,\mu}^{\text{alf}}(w))}{\sqrt{\frac{d}{dw}\psi_{\nu,\mu}^{\text{alf}}(w)}} &= \sqrt{\frac{\pi}{2\nu+1}} \cos(\pi(\mu+1)) \tilde{P}_{\nu}^{\mu}(\tanh(w)) \\ &\quad - \sqrt{\frac{\pi}{2\nu+1}} \sin(\pi(\mu+1)) \tilde{Q}_{\nu}^{\mu}(\tanh(w)) \end{aligned} \quad (201)$$

and

$$\begin{aligned} \frac{\cos(\psi_{\nu,\mu}^{\text{alf}}(w))}{\sqrt{\frac{d}{dw}\psi_{\nu,\mu}^{\text{alf}}(w)}} &= \sqrt{\frac{\pi}{2\nu+1}} \cos(\pi(\mu+1)) \tilde{P}_{\nu}^{\mu}(\tanh(w)) \\ &\quad + \sqrt{\frac{\pi}{2\nu+1}} \sin(\pi(\mu+1)) \tilde{Q}_{\nu}^{\mu}(\tanh(w)). \end{aligned} \quad (202)$$

In our first experiment, we sampled $l = 200$ equispaced points x_1, \dots, x_l in the interval $[1, 7]$. Then, for each $\nu = 10^{x_1}, \dots, 10^{x_l}$ and each $m = 10, 10^2, 10^3, 10^4$, we constructed the phase function $\psi_{m+\nu,m}^{\text{alf}}$ and applied the adaptive Levin method to the integral

$$(-1)^{m+1} \sqrt{\frac{2\nu+2m+1}{\pi}} \int_0^{\infty} \frac{\sin(\psi_{m+\nu,m}^{\text{alf}}(w))}{\sqrt{\frac{d}{dw}\psi_{m+\nu,m}^{\text{alf}}(w)}} \operatorname{sech}(w)^{2+m} dw \quad (203)$$

in order to evaluate $I_{15}(m + \nu, m)$. We note that the associated Legendre functions are generally only defined when the degree is greater than or equal

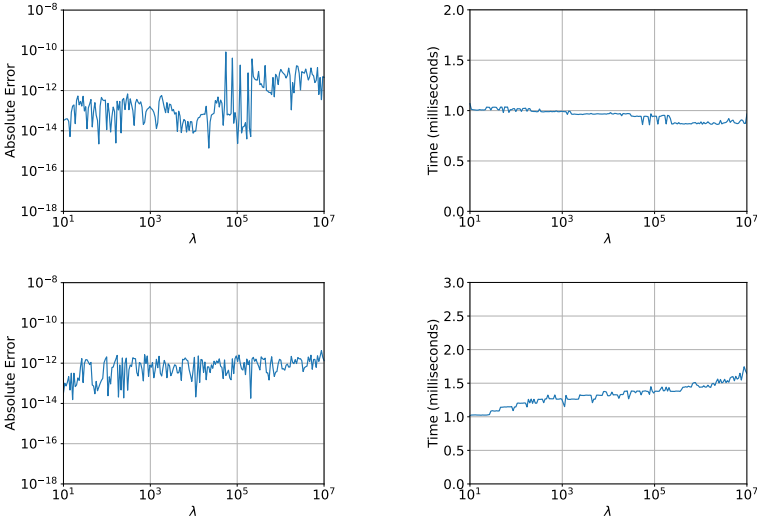


Fig. 7: The results of the last two experiments of Section 6.5. The first row pertains to $I_{16}(\lambda)$ while the second concerns $I_{17}(\lambda)$. In each row, the plot on the left gives the absolute error in the calculation of the integral as a function of λ and the plot on the right shows the total time required to compute the integral via the adaptive Levin method and to construct any necessary phase functions as a function of λ .

to the order, hence our decision to write the degree in the form $m + \nu$ with m the order of the associated Legendre function being integrated. Moreover, by choosing integer values of m we ensured that only the term involving the function of the first kind was nonzero in (201). The results are given in Figure 6. The timings reported there include both the cost to apply the adaptive Levin method and the time required to construct the phase function.

In our second experiment concerning the associated Legendre functions, we sampled $l = 200$ equispaced points x_1, \dots, x_l in the interval $[1, 7]$. Then, for each $\lambda = 10^{x_1}, \dots, 10^{x_l}$, we constructed the phase function $\psi_{\lambda, \frac{1}{2}}^{\text{alf}}$ and applied the adaptive Levin method to the integral

$$\frac{2\lambda + 1}{2\pi} \int_0^\infty \frac{\sin\left(2\psi_{\lambda, \frac{1}{2}}^{\text{alf}}(w)\right)}{\frac{d}{dw}\psi_{\lambda, \frac{1}{2}}^{\text{alf}}(w)} \operatorname{sech}(w)^2 dw, \quad (204)$$

which is equal to $I_{16}(\lambda)$ by virute of the fact that $\sin(2x) = 2\sin(x)\cos(x)$. We took the input functions for the adaptive Levin method to be

$$g(x) = 2\psi_{\lambda, \frac{1}{2}}^{\text{alf}}(x) \quad (205)$$

and

$$f(x) = \frac{2\lambda + 1}{2\pi} \frac{1}{\psi_{\lambda, \frac{1}{2}}^{\text{alf}}(\operatorname{arctanh}(\cos(x)))}. \quad (206)$$

The results are given in the first row of Figure 7. The timings reported there include both the cost to apply the adaptive Levin method and the time required to construct the required phase function.

In our third and final experiment regarding the associated Legendre functions, we sampled $l = 200$ equispaced points x_1, \dots, x_l in the interval $[1, 7]$. Then, for each $\lambda = 10^{x_1}, \dots, 10^{x_l}$, we constructed the phase function $\psi_{\lambda, 1}^{\text{alf}}$ via the algorithm of [15] and evaluated the integral $I_{17}(\lambda)$ via the adaptive Levin method. The input functions were taken to be

$$g(x) = \psi_{\lambda, 1}^{\text{alf}}(\operatorname{arctanh}(\cos(x))) \quad (207)$$

and

$$f(x) = \sqrt{\frac{2\lambda + 1}{2\pi}} \frac{1}{\sqrt{\psi_{\lambda, 1}^{\text{alf}}(\operatorname{arctanh}(\cos(x)))}}. \quad (208)$$

The results are shown in the second row of Figure 7. The timings reported there include both the cost to apply the adaptive Levin method and the time required to construct the required phase function.

6.6 Certain integrals involving the Hermite polynomials

In the experiments of this subsection, we used the adaptive Levin method to evaluate the integrals

$$\begin{aligned} I_{18}(n) &= \int_0^\infty \tilde{H}_n(x) \exp\left(\frac{-x^2}{2}\right) dx, \\ I_{19}(n) &= \int_0^\infty \tilde{H}_n(x)(x) \cos(nx) \exp(-x) dx \quad \text{and} \\ I_{20}(n) &= \int_0^\infty \tilde{H}_n(\exp(x)) dx, \end{aligned}$$

where \tilde{H}_n denotes a normalized version of the Hermite polynomial of degree n . The Hermite polynomial H_n is the unique solution of

$$y''(x) - 2xy'(x) + 2ny(x) = 0 \quad (209)$$

which decays to 0 as $x \rightarrow \pm\infty$ and such that

$$H_n(0) = \frac{2^n \sqrt{\pi}}{\Gamma\left(\frac{1-n}{2}\right)}. \quad (210)$$

We define \tilde{H}_n via

$$\tilde{H}_n(x) = \sqrt{\frac{\Gamma(n+1)}{2^n \sqrt{\pi}}} \exp\left(-\frac{x^2}{2}\right) H_n(x); \quad (211)$$

it is a solution of

$$y''(x) + (1 + 2n - x^2) y(x) = 0 \quad (212)$$

whose $L^2(-\infty, \infty)$ norm is 1. Applying the algorithm of [15] to (212) gives us the representation

$$\tilde{H}_n(x) = C_n^{\text{herm}} \frac{\sin(\psi_n^{\text{herm}}(x))}{\sqrt{\frac{d}{dx} \psi_n^{\text{herm}}(x)}} \quad (213)$$

of the normalized Hermite polynomial of degree n . The authors are not aware of a convenient formula for the constant C_n^{herm} ; we determine it numerically after the phase function has been constructed.

In our first experiment, we sampled $l = 200$ equispaced points x_1, \dots, x_l in the interval $[1, 7]$. Then, for each $n = \lfloor 10^{x_1} \rfloor, \dots, \lfloor 10^{x_l} \rfloor$, we constructed the phase function ψ_n^{herm} and used it to evaluate $I_{18}(n)$. The results are given in the first row of Figure 8. The timings reported there include both the cost to apply the adaptive Levin method and the time required to construct the phase function.

In a second experiment concerning Hermite polynomials, we sampled $l = 200$ equispaced points x_1, \dots, x_l in the interval $[1, 7]$. Then, for each $n = \lfloor 10^{x_1} \rfloor, \dots, \lfloor 10^{x_l} \rfloor$, we constructed the phase function ψ_n^{herm} and used it to evaluate the integrals

$$I_{19a}(n) = \int_0^\infty \frac{\sin(\psi_n^{\text{herm}}(x) - nx)}{\sqrt{\frac{d}{dx} \psi_n^{\text{herm}}(x)}} \exp(-x) dx \quad (214)$$

and

$$I_{19b}(n) = \int_0^\infty \frac{\sin(\psi_n^{\text{herm}}(x) + nx)}{\sqrt{\frac{d}{dx} \psi_n^{\text{herm}}(x)}} \exp(-x) dx \quad (215)$$

The value of $I_{19}(n)$ is then given by

$$I_{19}(n) = C_n^{\text{herm}} \frac{I_{19a}(n) + I_{19b}(n)}{2} \quad (216)$$

since

$$\sin(x) \cos(y) = \frac{\sin(x - y) + \sin(x + y)}{2}. \quad (217)$$

The results of this experiment are given in the second row of Figure 8. Again, the reported timings include both the cost to apply the adaptive Levin method and the time required to construct the phase function.

We began our third and final experiment regarding the Hermite polynomials by sampling $l = 200$ equispaced points x_1, \dots, x_l in the interval $[1, 7]$. Then, for each $n = \lfloor 10^{x_1} \rfloor, \dots, \lfloor 10^{x_l} \rfloor$, we constructed the phase function ψ_n^{herm} and used it to evaluate $I_{20}(n)$. We took the input functions for the adaptive Levin method to be

$$g(x) = \psi_n^{\text{herm}}(\exp(x)) \quad \text{and} \quad f(x) = C_n^{\text{herm}} \frac{1}{\sqrt{\frac{d}{dx} \psi_n^{\text{herm}}(\exp(x))}}. \quad (218)$$

The results are shown in the third row of Figure 8. The timings reported there include both the cost to apply the adaptive Levin method and the time required to construct the phase function.

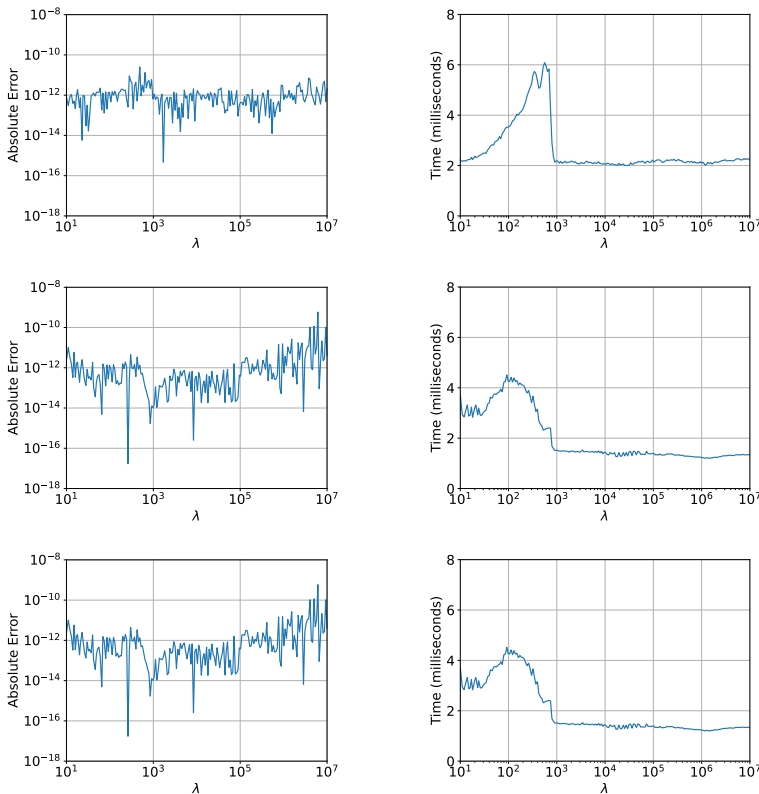


Fig. 8: The results of the experiments of Section 6.6. The first row pertains to $I_{18}(\lambda)$, the second concerns $I_{19}(\lambda)$ and the third pertains to $I_{20}(\lambda)$. In each row, the plot on the left gives the absolute error in the calculation of the integral as a function of λ and the plot on the right shows the total time required to compute the integral via the adaptive Levin method and to construct any necessary phase functions as a function of λ .

6.7 Evaluation of Modal Green's functions

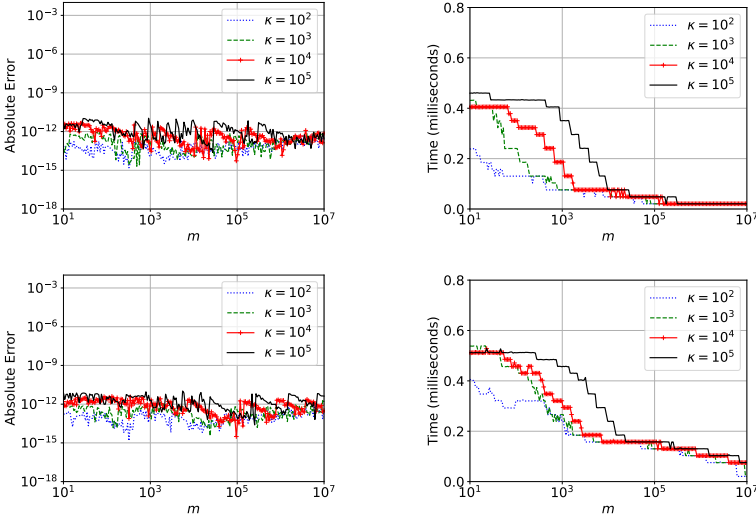


Fig. 9: The results of the first experiment of Section 6.7. The plot on the left-hand side of the first row gives the absolute error in the calculated value of $I_{21}(\kappa, m, \alpha)$ as a function of m for four values of κ in the case $\alpha = 0.5$. The plot on the right-hand side of the first row gives the time required to calculate $I_{21}(\kappa, m, \alpha)$ via the adaptive Levin method as a function of m for four values of κ in the case $\alpha = 0.5$. The plots in the second row give analogous data in the event $\alpha = 0.99$.

In this set of experiments, we used the adaptive Levin method to evaluate the azimuthal Fourier components of the Green's function

$$G(x, x') = \frac{\exp(ik|x - x'|)}{4\pi|x - x'|} \quad (219)$$

for the Helmholtz equation in three dimensions. These functions, which are known as the modal Green's functions for the Helmholtz equation, are given by

$$\frac{1}{2\pi} \int_{-\pi}^{\pi} \frac{\exp(ik|x - x'|)}{4\pi|x - x'|} \exp(-im\theta) d\theta. \quad (220)$$

By introducing cylindrical coordinates $x = (r, \theta, z)$, $x' = (r', \theta', z')$ and letting $\phi = \theta - \theta'$, we can rewrite (220) as

$$I_{21}(\kappa, m, \alpha) = \frac{1}{4\pi^2} \int_{-\pi}^{\pi} \frac{\exp\left(-i\kappa\sqrt{1 - \alpha\cos(\phi)}\right)}{\sqrt{1 - \alpha\cos(\phi)}} \cos(m\phi) d\phi, \quad (221)$$

where

$$\kappa = kR_0, \quad \alpha = \frac{2rr'}{R_0^2}, \quad \text{and} \quad R_0^2 = r^2 + (r')^2 + (z - z')^2. \quad (222)$$

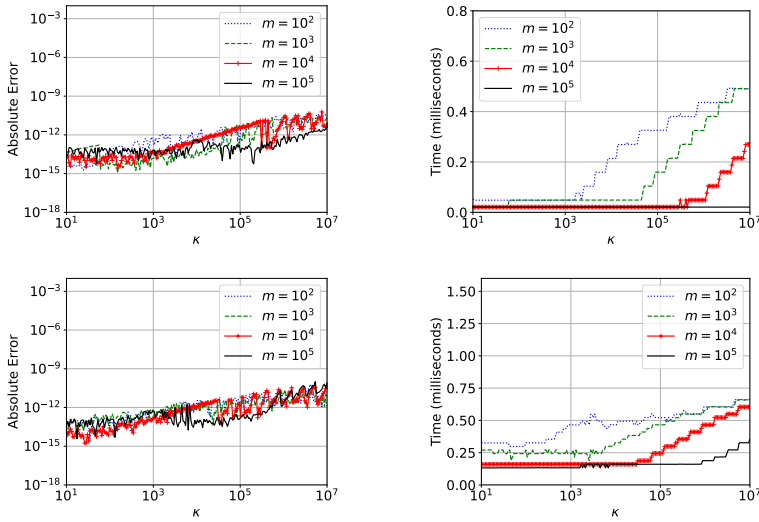


Fig. 10: The results of the second experiment of Section 6.7. The plot on the left-hand side of the first row gives the absolute error in the calculated value of $I_{21}(\kappa, m, \alpha)$ as a function of κ for four values of m in the case $\alpha = 0.5$. The plot on the right-hand side of the first row gives the time required to calculate $I_{21}(\kappa, m, \alpha)$ via the adaptive Levin method as a function of κ for four values of m in the case $\alpha = 0.5$. The plots in the second row give analogous data in the event $\alpha = 0.99$.

In the first experiment, we sampled $l = 200$ equispaced points x_1, \dots, x_l in the interval $[1, 7]$. Then, for each $m = 10^{x_1}, \dots, 10^{x_l}$, $\kappa = 10^2, 10^3, 10^4, 10^5$ and $\alpha = 0.5, 0.99$ we evaluated $I_{21}(\kappa, m, \alpha)$ using the adaptive Levin method and via adaptive Gaussian quadrature. Figure 9 gives the results.

In a second experiment, we sampled $l = 200$ equispaced points x_1, \dots, x_l in the interval $[1, 7]$. Then, for each $\kappa = 10^{x_1}, \dots, 10^{x_l}$, $m = 10^2, 10^3, 10^4, 10^5$ and $\alpha = 0.5, 0.99$ we evaluated $I_{21}(\kappa, m, \alpha)$ using the adaptive Levin method and via adaptive Gaussian quadrature. In this experiment, the tolerance parameters for both the adaptive Levin method and our adaptive Gaussian quadrature code were set to $\epsilon_0 \sqrt{\kappa}$, where ϵ_0 is machine zero for IEEE double precision arithmetic (about 2.22×10^{-16}). The value of $I_{21}(\kappa, m, \alpha)$ decreases, but not at a sufficient rate to completely compensate for the growth in its condition number, particularly when α is close to 1. Hence, the need to allow the tolerance parameter to increase with κ . Figure 10 gives the results.

A state-of-the-art method for evaluating the modal Green's functions is discussed in [25]. It is more efficient than the adaptive Levin method in all cases, and it is much faster when α is close to 1. However, the adaptive Levin method is surprisingly competitive given that it is a general-purpose approach to evaluating oscillatory integrals and the algorithm of [25] is highly-specialized.

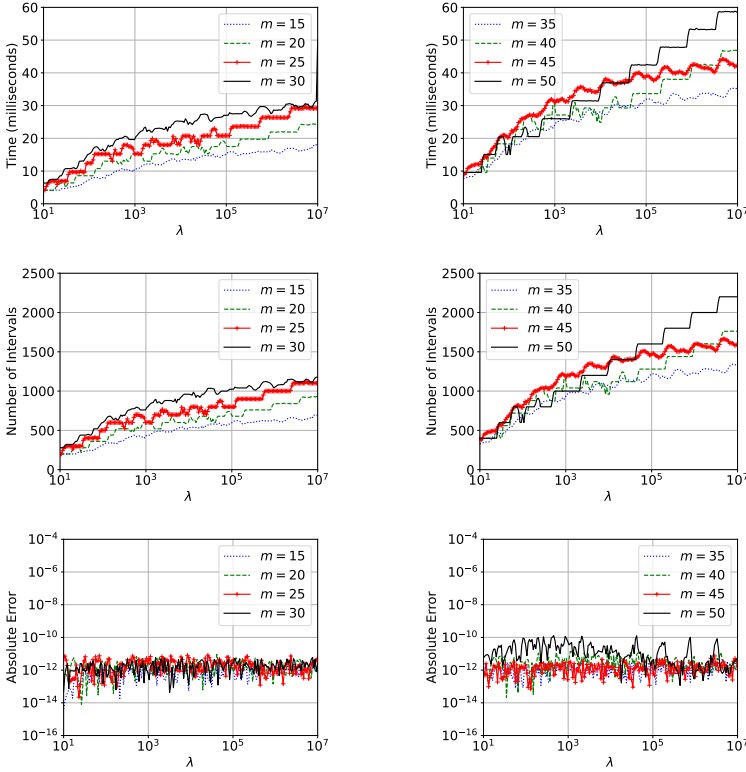


Fig. 11: The results of the experiment of Section 6.8. The plots in the first row give the time taken by the adaptive Levin method as a function of λ for the various values of m considered. Those in the second row give the number of intervals in the adaptively determined subdivision of $[-1, 1]$ used to compute the integral I_{22} as a function of λ for the values of m considered. The third row of plots give the error in the calculated value of $I_{22}(\lambda, m)$ as a function of λ for $m = 15, 20, 25, 30, 35, 40, 45, 50$.

6.8 An integral with many stationary points

In this final experiment, we considered the integral

$$I_{22}(\lambda, m) = \int_{-1}^1 \exp\left(i\lambda \cos^2\left(\frac{\pi}{2}mx\right)\right) \frac{1}{1+x^2} dx, \quad (223)$$

which has m stationary points. We sampled $l = 200$ equispaced points x_1, \dots, x_l in the interval $[1, 7]$ and, for each $\lambda = 10^{x_1}, 10^{x_2}, \dots, 10^{x_l}$ and $m = 15, 20, 25, 30, 35, 40, 45, 50$, we evaluated $I_{22}(\lambda, m)$ using the adaptive Levin method.

Figure 11 presents the results. We see that, when applied to I_{22} , the running time of the adaptive Levin method grows sublogarithmically with λ for all of the values of m considered. The cost also increases quite mildly as a function

of the number of stationary points. It is notable that the method is able to evaluate $I_{22}(10^7, 20)$ — a highly oscillatory integral with 50 stationary points — to 11 digit accuracy in approximately 50 milliseconds.

7 Conclusions

We have shown that the Levin method does not suffer from numerical breakdown when the magnitude of g' is small or when g' has zeros, which explains the effectiveness of adaptive Levin methods. We have also presented numerical experiments indicating that the adaptive Levin method of this paper can accurately and rapidly evaluate a large class of oscillatory integrals, including many with singularities and stationary points. We have further demonstrated that combining the adaptive Levin method with the algorithm of [14, 13] allows for the efficient evaluation of many integrals involving the solutions of differential equations. This class includes integrals involving most of the classical special functions, as well combinations of such functions.

As the experiments of Section 6.7 indicate, specialized techniques designed for particular narrow classes of oscillatory integrals are often faster than the adaptive Levin scheme of this paper. However, the numerical experiments described in Section 6 show that the adaptive Levin method provides an efficient general-purpose mechanism for evaluating a huge class of oscillatory integrals. It appears to have the roughly the same behavior when applied to oscillatory integrals as adaptive Gaussian quadrature does when used to evaluate smoothly varying integrands.

We note that there are obvious implications of the adaptive Levin method for the rapid application of special function transforms and the solution of second order linear inhomogeneous differential equations that should be thoroughly investigated.

8 Acknowledgements

KS was supported in part by the NSERC Discovery Grants RGPIN-2020-06022 and DGECR-2020-00356. JB was supported in part by NSERC Discovery grant RGPIN-2021-02613.

References

- [1] Levin, D.: Procedures for computing one- and two-dimensional integrals of functions with rapid irregular oscillations. *Mathematics of Computation* **38**, 531–538 (1982)
- [2] Li, J., Wang, X., Wang, T.: A universal solution to one-dimensional oscillatory integrals. *Science in China Series F: Information Sciences* **51**, 1614–1622 (2008)

- [3] Li, J., Wang, X., Wang, T., Xiao, S.: An improved Levin quadrature method for highly oscillatory integrals. *Applied Numerical Mathematics* **60**(8), 833–842 (2010)
- [4] Levin, D.: Analysis of a collocation method for integrating rapidly oscillatory functions. *Journal of Computational and Applied Mathematics* **78**(1), 131–138 (1997)
- [5] Moylan, A.J.: Highly oscillatory integration, numerical wave optaions, and the gravitational lensing of gravitational waves. PhD thesis, The Australian National University (2008)
- [6] Levin, D.: Fast integration of rapidly oscillatory functions. *Journal of Computational and Applied Mathematics* **67**, 95–101 (1996)
- [7] Miller, P.D.: *Applied Asymptotic Analysis*. American Mathematical Society, Providence, Rhode Island (2006)
- [8] Wasow, W.: *Asymptotic Expansions for Ordinary Differential Equations*. Dover, New York (1965)
- [9] Spigler, R., Vianello, M.: The phase function method to solve second-order asymptotically polynomial differential equations. *Numerische Mathematik* **121**, 565–586 (2012)
- [10] Spigler, R.: Asymptotic-numerical approximations for highly oscillatory second-order differential equations by the phase function method. *Journal of Mathematical Analysis and Applications* **463**, 318–344 (2018)
- [11] Spigler, R., Vianello, M.: A numerical method for evaluating the zeros of solutions of second-order linear differential equations. *Mathematics of Computation* **55**, 591–612 (1990)
- [12] Bremer, J., Rokhlin, V.: Improved estimates for nonoscillatory phase functions. *Discrete and Continuous Dynamical Systems, Series A* **36**, 4101–4131 (2016)
- [13] Aubry, M., Bremer, J.: A solver for linear scalar ordinary differential equations whose running time is bounded independent of frequency. *arXiv:2311.08578* (2023)
- [14] Bremer, J.: On the numerical solution of second order differential equations in the high-frequency regime. *Applied and Computational Harmonic Analysis* **44**, 312–349 (2018)
- [15] Bremer, J.: Phase function methods for second order linear ordinary differential equations with turning points. *Applied and Computational Harmonic Analysis* **65**, 137–169 (2023). <https://doi.org/10.1016/j.acha.2023.02.005>
- [16] Mason, J.C., Hanscomb, D.C.: *Chebyshev Polynomials*. Chapman and Hall, New York, New York (2003)

52 REFERENCES

- [17] Boyd, J.P.: Approximation of an analytic function on a finite real interval by a bandlimited function and conjectures on properties of prolate spheroidal functions. *Applied and Computational Harmonic Analysis* **15**(2), 168–176 (2003)
- [18] Davis, P.: *Interpolation and Approximation*. Dover, New York, New York (1975)
- [19] *NIST Digital Library of Mathematical Functions*. <http://dlmf.nist.gov/>, Release 1.1.0 of 2020-12-15. F. W. J. Olver, A. B. Olde Daalhuis, D. W. Lozier, B. I. Schneider, R. F. Boisvert, C. W. Clark, B. R. Miller, B. V. Saunders, H. S. Cohl, and M. A. McClain, eds. <http://dlmf.nist.gov/>
- [20] Bateman, H., Erdélyi, A.: *Higher Transcendental Functions* vol. II. McGraw-Hill, New York, New York (1953)
- [21] Zhao, M., Serkh, K.: On the approximation of singular functions by series of non-integer powers. arXiv:2308.10439 (2023)
- [22] Gradshteyn, I.S., Ryzhik, I.M.: *Table of Integrals, Sums, Series and Products*, 7th edn. Academic Press, Amsterdam (2007)
- [23] Bateman, H., Erdélyi, A.: *Tables of Integrals* vol. II. McGraw-Hill, New York, New York (1954)
- [24] Olver, F.W.J.: *Asymptotics and Special Functions*. A.K. Peters, Wellesley, Massachusetts (1997)
- [25] Garritano, J., Kluger, Y., Rokhlin, V., Serkh, K.: On the efficient evaluation of the azimuthal Fourier components of the Green’s function for Helmholtz’s equation in cylindrical coordinates. arXiv 2104.12241 (2021)